Super Nested Arrays: Linear Sparse Arrays With Reduced Mutual Coupling—Part I: Fundamentals

Chun-Lin Liu, *Student Member, IEEE*, and P. P. Vaidyanathan, *Fellow, IEEE*

***Abstract*—In array processing, mutual coupling between sensors has an adverse effect on the estimation of parameters (e.g., DOA). While there are methods to counteract this through appropriate modeling and calibration, they are usually computationally expensive, and sensitive to model mismatch. On the other hand, sparse arrays, such as nested arrays, coprime arrays, and minimum redundancy arrays (MRAs), have reduced mutual coupling compared to uniform linear arrays (ULAs). With N denoting the number of sensors, these sparse arrays offer $O(N^2)$ freedoms for source estimation because their difference coarrays have $O(N^2)$-long ULA segments. But these well-known sparse arrays have disadvantages: MRAs do not have simple closed-form expressions for the array geometry; coprime arrays have holes in the coarray; and nested arrays contain a dense ULA in the physical array, resulting in significantly higher mutual coupling than coprime arrays and MRAs. This paper introduces a new array called the super nested array, which has all the good properties of the nested array, and at the same time achieves reduced mutual coupling. There is a systematic procedure to determine sensor locations. For fixed N, the super nested array has the same physical aperture, and the same hole-free coarray as does the nested array. But the number of sensor pairs with small separations ($\lambda/2$, $2\times\lambda/2$, etc.) is significantly reduced. Many theoretical properties are proved and simulations are included to demonstrate the superior performance of these arrays. In the companion paper, a further extension called the Qth-order super nested array is developed, which further reduces mutual coupling.**

***Index Terms*—Sparse arrays, nested arrays, coprime arrays, super nested arrays, mutual coupling, DOA estimation.**

I. Introduction

ARRAY processing plays a significant role in many applications such as radar [1], astronomy [2], tomography [2], and communications [3]. Sensor measurements enable us to extract source profiles, such as direction-of-arrival (DOA), radial velocity, range, power, and polarization [1]–[4]. However, in practice, electromagnetic characteristics cause *mutual coupling* between sensors, making the sensor responses interfere with each other [1], [5]. This has an adverse effect on the estimation of parameters (e.g., DOA). State-of-the-art approaches aim to *decouple* (or "remove") the effect of mutual coupling from the received data by using *proper* mutual coupling models [1]–[15]. Such methods are usually computationally expensive, and sensitive to model mismatch.

An altogether different approach to reduce the effect of mutual coupling is to use sparse arrays, in which the number of sensor pairs with small separations (small multiples of $\lambda/2$) is much fewer than in uniform linear arrays (ULAs). This paper is based on this theme. Sparse arrays such as nested arrays, coprime arrays [16]–[20], minimum redundancy arrays (MRAs) [21] and minimum hole arrays (MHAs) [22], [23] have reduced mutual coupling compared to ULAs. They also offer another important advantage over ULAs: with N denoting the number of sensors, these sparse arrays offer $O(N^2)$ freedoms for source estimation because their difference coarrays have $O(N^2)$-long ULA segments [16], [17]. That is, the number of uncorrelated source directions that can be estimated is increased from $N-1$ to $O(N^2)$. Typically a MUSIC algorithm is performed in the difference coarray domain to achieve this [16], [17].

In practice, these well-known sparse arrays have some shortcomings: MRAs and MHAs do not have simple closed-form expressions for the array geometry, and the sensor locations are usually found from tabulated entries [21]–[24]. Coprime arrays have holes in the coarray, so that the ULA part of the coarray is smaller than those of the nested array and the MRA [17]. Finally nested arrays, by definition, contain a dense ULA in the physical array, resulting in significantly higher mutual coupling than coprime arrays and MRAs [16].

The main aim of this paper is to introduce a new array configuration called the *super nested array*, which has all the good properties of the nested array, and at the same time achieves reduced mutual coupling by redistributing the elements of the dense ULA part of the nested array. There is a systematic procedure to do this. We will show how to determine the appropriate sensor locations for any N. For fixed N (number of sensors), the super nested array has the same physical aperture as the parent nested array. Furthermore, its difference coarray is exactly identical to that of the nested array and is, in particular, free from holes. However, unlike the nested array, the number of sensor pairs with small separations ($\lambda/2, 2\times\lambda/2$, etc.) is significantly reduced. More quantitative statements of these properties will be given in this paper based on the weight function $w(m)$ of the sparse array (where $w(m)$ is the number of pairs of elements with element-spacing $m\lambda/2$). Several other properties of the new array geometry will also be established.

To explain how the super nested array is obtained from a nested array, it is first convenient to develop a two-dimensional (2D) representation of linear arrays. This is demonstrated in Fig. 1 which shows the traditional (1D) and the corresponding 2D representations of a nested array with $N_1 = N_2 = 5$ (N_1

Manuscript received September 10, 2015; revised February 02, 2016; accepted March 05, 2016. Date of publication April 25, 2016; date of current version June 24, 2016. This work was supported in part by the Office of Naval Research (ONR) under Grant N00014-15-1-2118, and the California Institute of Technology. The associate editor coordinating the review of this manuscript and approving it for publication was Prof. Amir Asif.

The authors are with the California Institute of Technology, Pasadena, CA 91125, USA (e-mail: cl.liu@caltech.edu; ppvnath@systems.caltech.edu).

Color versions of one or more of the figures in this paper are available online at http://ieeexplore.ieee.org.

Digital Object Identifier 10.1109/TSP.2016.2558159

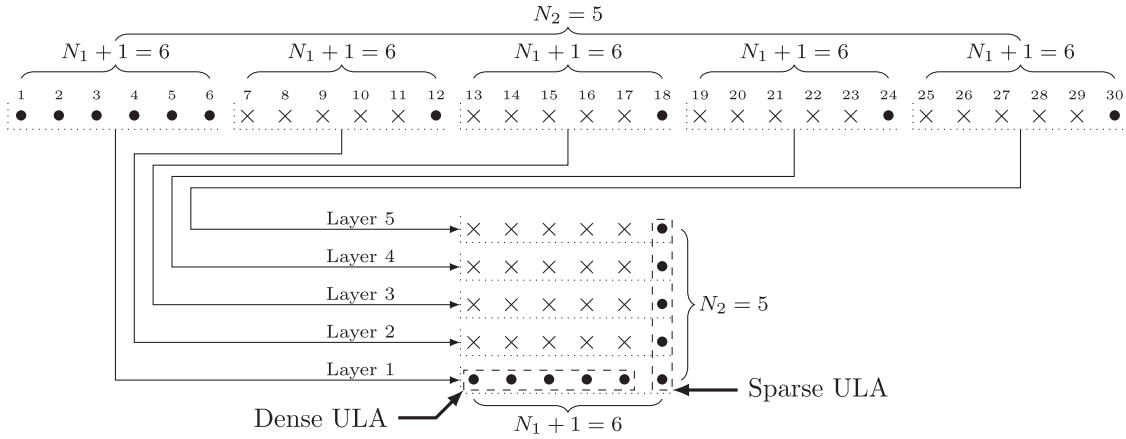

Fig. 1. The concept of 2D representations of linear arrays. The top of this figure shows the 1D representation of a nested array with $N_1 = N_2 = 5$, where bullets denote sensors and crosses indicate empty locations. In the 1D representation of this example, the array aperture is divided into $N_2 = 5$ layers of size $N_1 + 1 = 6$. These layers are stacked into the associated 2D representation, as marked by arrows. Notice that in this paper, 2D representations denote linear arrays, *not planar arrays*. They are introduced to simplify the discussion in the future development.

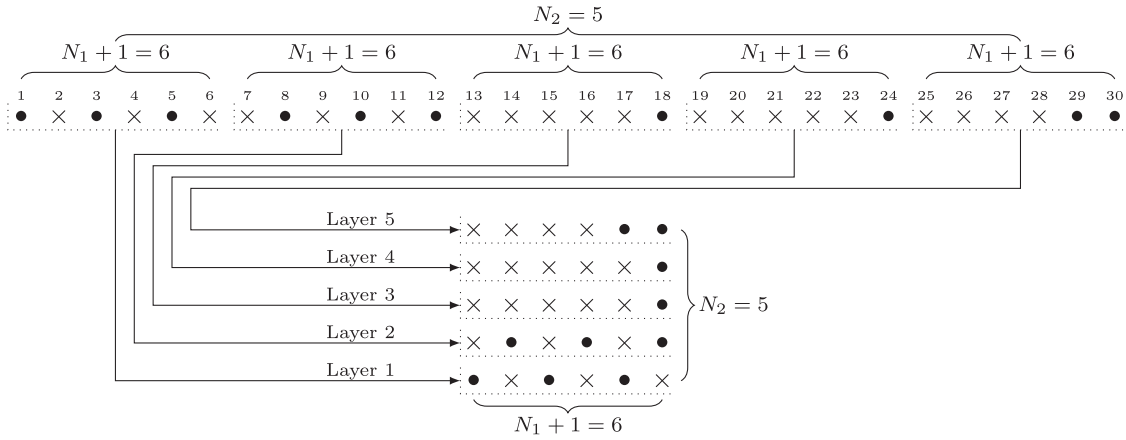

Fig. 2. The 1D and 2D representations of a second-order super nested array with $N_1 = N_2 = 5$. It will be proved in this paper that super nested arrays possess the same number of sensors, the same physical aperture, and the same hole-free coarray as their parent nested arrays. Furthermore, super nested arrays alleviate the mutual coupling effect. In this example, there is only one pair of sensors with separation 1, located at 29 and 30. However, for the parent nested array in Fig. 1, locations 1 through 6 are crowded with sensors, leading to more severe mutual coupling effect.

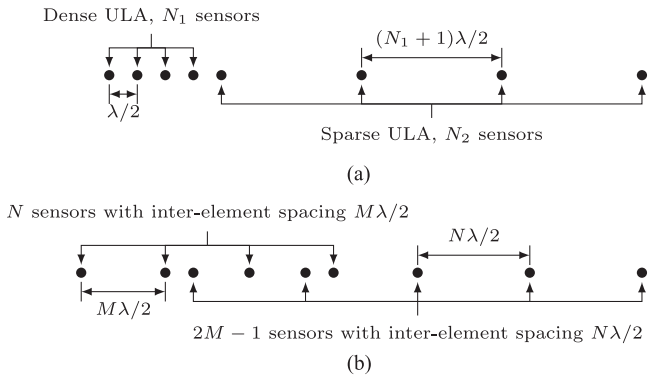

Fig. 3. 1D representations of (a) nested arrays and (b) coprime arrays.

and N_2 have the same meaning as in [16]; also see Fig. 3(a)). The top of Fig. 1 depicts this array configuration along an 1D axis, where bullets are physical sensors and crosses stand for empty space. *Layer* 1 is defined as the locations from 1 to $N_1 + 1 = 6$ while Layer 2 begins with $N_1 + 2 = 7$ and ends with $2(N_1 + 1) = 12$. The *2D representation* establishes a 2D topology by stacking all these layers, as illustrated in the bottom of Fig. 1. Then, the dense ULA and the sparse ULA structure of a nested array can be readily visualized. Note that in this paper, 2D representations denote linear arrays, *not planar arrays*.

Next, Fig. 2 provides a first glance at a second-order super nested array with parameters $N_1 = N_2 = 5$. These parameters are the same as those in Fig. 1. Hence, the array in Fig. 1 is said to be the *parent nested array* of the array in Fig. 2. It can be seen from this example that this super nested array is sparser than its parent nested array (for the same physical aperture) in the sense that the number of element pairs with small spacing (spacings of 1, 2, and 3) are reduced. In this super nested array, there is only one pair of sensors with separation 1, but in its parent nested array, five sensor pairs of separation 1 exist. We will see that such rearrangements will significantly reduce the adverse effects of mutual coupling in DOA estimation. Later

on, it will be shown in Fig. 8 that, with mutual coupling, the DOA estimation error for the (third-order) super nested array is as small as 2% of that for its parent nested array, which is truly remarkable.

Even though the 1D representation of super nested arrays seems irregular, their 2D representation provides a geometrical point of view, as shown in Fig. 2. It can be noticed that Fig. 2 resembles Fig. 1, except for few sensor locations. In this example, we start with the parent nested array in Fig. 1 and then relocate some sensors, from location 2 to 8, 4 to 10, and 6 to 29, yielding the super nested array in Fig. 2. The systematic construction of super nested arrays from nested arrays for arbitrary N_1 and N_2 will be described more rigorously in Section IV.

A. Paper Outline

Section II reviews sparse array processing and mutual coupling models. In Section III, we present a motivating example which compares the performances of well-known sparse arrays in the presence of mutual coupling. Super nested arrays are then introduced in Section IV, and some of their basic properties are proved (Lemma 1 and Lemma 2). In Section V, we study the difference coarray of the super nested array in detail. It will be proved that super nested arrays have the same hole-free coarray as their parent nested arrays (Theorem 1, and Corollary 1). Furthermore, a closed-form expression for the weight function $w(m)$ of the super nested array is provided in Theorem 2. The first three weights (which dominate the effects of mutual coupling) are shown to be always smaller for the super nested array, compared to the parent nested array ($w(1)$ and $w(3)$ being *significantly* smaller). The improved performance of super nested arrays under mutual coupling will be demonstrated through examples in Section VI. Section VII concludes this paper.

A MATLAB code to generate the sensor locations of the super nested array can be found in [25]. This code takes N_1 and N_2 (which are defined by the parent nested array as in Fig. 3(a)) as the inputs and returns the sensor locations as the output.

The arrays introduced in this paper will be called *second-order* super nested arrays, for reasons that will become clear soon. In the companion paper, a further extension called the Qth-order super nested array is developed, which further reduces mutual coupling.

II. Preliminaries

A. Sparse Array Processing

Assume D monochromatic far-field sources impinge on the sensor array, where the sensor locations are nd. Here n belongs to some integer set $\mathbb{S}$ and $d = \lambda/2$ denotes the minimum distance between sensors. For the ith source, its complex amplitude is written as A_i and its direction-of-arrival (DOA) is denoted by $\theta_i \in [-\pi/2, \pi/2]$. The measurement vector $\mathbf{x}_{\mathbb{S}}$ on the sensor array $\mathbb{S}$ can be modeled as follows:

$$\mathbf{x}_{\mathbb{S}} = \sum_{i=1}^{D} A_i \mathbf{v}_{\mathbb{S}}\left(\overline{\theta}_i\right) + \mathbf{n}_{\mathbb{S}}, \tag{1}$$

where $\mathbf{v}_{\mathbb{S}}(\overline{\theta}_i) = [e^{j2\pi\overline{\theta}_i n}]_{n\in\mathbb{S}}$ are steering vectors and $\mathbf{n}_{\mathbb{S}}$ is the additive noise term. $\overline{\theta}_i = (d/\lambda)\sin\theta_i$ is the normalized DOA. We obtain $-1/2 \le \overline{\theta} \le 1/2$. The parameters A_i and $\mathbf{n}_{\mathbb{S}}$ are assumed to be zero-mean, uncorrelated random variables with $\mathbb{E}[A_i A_j^*] = \sigma_i^2\delta_{i,j}$ and $\mathbb{E}[\mathbf{n}_{\mathbb{S}}\mathbf{n}_{\mathbb{S}}^H] = \sigma^2\mathbf{I}$. Here σ_i^2 is the power of the ith source, σ^2 is the noise power, and $\delta_{p,q}$ is the Kronecker delta. $\overline{\theta}_i$ is considered to be fixed but unknown.

Here we briefly review the bracket notation in sparse array processing. Consider an example of a sensor array with three elements. The first, second, and third elements are located at $d, 3d$, and $5d$, respectively. After normalizing by d, the sensor locations can be specified by the following integer set: $\mathbb{S} = \{1, 3, 5\}$. Assume that the signals received by the first, second, and third sensor are -2, -5, and -10, respectively. These signals can be modeled as a column vector $\mathbf{x}_{\mathbb{S}} = [-2, -5, -10]^T$. The square brackets $[\mathbf{x}_{\mathbb{S}}]_i$ indicate the ith component of $\mathbf{x}_{\mathbb{S}}$, i.e., the signal received by the ith sensor. We write $[\mathbf{x}_{\mathbb{S}}]_1 = -2, [\mathbf{x}_{\mathbb{S}}]_2 = -5$, and $[\mathbf{x}_{\mathbb{S}}]_3 = -10$. The angle brackets $\langle\mathbf{x}_{\mathbb{S}}\rangle_n$ represent the value of the signal at the sensor location nd. That is, $\langle\mathbf{x}_{\mathbb{S}}\rangle_1 = -2, \langle\mathbf{x}_{\mathbb{S}}\rangle_3 = -5$, and $\langle\mathbf{x}_{\mathbb{S}}\rangle_5 = -10$. These notations apply to covariance matrices as $[\mathbf{R}_{\mathbb{S}}]_{i,j} = \mathbb{E}[[\mathbf{x}_{\mathbb{S}}]_i[\mathbf{x}_{\mathbb{S}}]_j^*]$ and $\langle\mathbf{R}_{\mathbb{S}}\rangle_{n,m} = \mathbb{E}[\langle\mathbf{x}_{\mathbb{S}}\rangle_n\langle\mathbf{x}_{\mathbb{S}}\rangle_m^*]$.

The covariance matrix of $\mathbf{x}_{\mathbb{S}}$ can be expressed as

$$\mathbf{R}_{\mathbb{S}} = \sum_{i=1}^{D} \sigma_i^2 \mathbf{v}_{\mathbb{S}}(\overline{\theta}_i)\mathbf{v}_{\mathbb{S}}^H(\overline{\theta}_i) + \sigma^2\mathbf{I}. \tag{2}$$

Since the entries in $\mathbf{v}_{\mathbb{S}}(\overline{\theta}_i)\mathbf{v}_{\mathbb{S}}^H(\overline{\theta}_i)$ are of the form $e^{j2\pi\overline{\theta}_i(n_1-n_2)}$, where $n_1, n_2 \in \mathbb{S}$, it enables us to reshape (2) into an autocorrelation vector $\mathbf{x}_{\mathbb{D}}$ as in [16] , [26]

$$\mathbf{x}_{\mathbb{D}} = \sum_{i=1}^{D} \sigma_i^2 \mathbf{v}_{\mathbb{D}}\left(\overline{\theta}_i\right) + \sigma^2\mathbf{e}_0, \tag{3}$$

where $\langle\mathbf{e}_0\rangle_n = \delta_{n,0}$ for $n \in \mathbb{D}$.

Definition 1 (Difference Coarray): For a sparse array specified by an integer set $\mathbb{S}$, its difference coarray $\mathbb{D}$ is defined as

$$\mathbb{D} = \{n_1 - n_2 | n_1, n_2 \in \mathbb{S}\}.$$

In other words, the original model (1) in the physical array domain $\mathbb{S}$, is converted into another model (3) in the difference coarray domain $\mathbb{D}$. According to $\mathbb{D}$, we define the following terminologies:

Definition 2 (Degrees of Freedom): The number of degrees of freedom (DOF) of a sparse array $\mathbb{S}$ is the cardinality of its difference coarray $\mathbb{D}$.

Definition 3 (Uniform DOF): Given an array $\mathbb{S}$, let $\mathbb{U}$ denote the central ULA segment of its difference coarray. The number of elements in $\mathbb{U}$ is called the number of uniform degrees of freedom or "uniform DOF" of $\mathbb{S}$.

If the uniform DOF is $\mathcal{F}$, then the number of uncorrelated sources that can be identified by using coarray MUSIC is $(\mathcal{F}-1)/2$ [16], [26].

Definition 4 (Restricted Arrays [21]): A restricted array is an array whose difference coarray $\mathbb{D}$ is a ULA with adjacent elements separated by $\lambda/2$. In other words, there are no holes in the coarray domain. Thus the phrase "restricted array"is equivalent to "array with hole-free difference coarray."

Definition 5 (General Arrays [21]): If the difference coarray $\mathbb{D}$ of a sparse array $\mathbb{S}$ is not a ULA with inter-element spacing $\lambda/2$, then it is a general array.

For instance, if $\mathbb{S}=\{1,2,4\}$, the corresponding difference coarray becomes $\mathbb{D}=\{-3,-2,-1,0,1,2,3\}$ and the maximum contiguous ULA segment of $\mathbb{D}$ is exactly $\mathbb{D}$. Therefore, its DOF and uniform DOF are both 7, implying that $\mathbb{S}$ is a restricted array. However, $\mathbb{S}=\{1,2,5\}$ results in $\mathbb{D}=\{-4,-3,-1,0,1,3,4\}$ and the maximum ULA section $\mathbb{U}=\{-1,0,1\}$. The associated DOF and uniform DOF are 7 and 3, respectively. This array is a general array. As another example, nested arrays are restricted arrays [16] while coprime arrays are general arrays [17], [26].

In the finite-snapshot setting, where the measurement vectors $\widetilde{\mathbf{x}}_{\mathbb{S}}(k), k=1,2,...,K$ are given, the covariance matrix can be estimated by

$$\widetilde{\mathbf{R}}_{\mathbb{S}}=\frac{1}{K}\sum_{k=1}^{K}\widetilde{\mathbf{x}}_{\mathbb{S}}\left(k\right)\widetilde{\mathbf{x}}_{\mathbb{S}}^{H}\left(k\right).$$

The finite-snapshot version of the autocorrelation function can be averaged from the covariance matrix by

$$\langle\widetilde{\mathbf{x}}_{\mathbb{D}}\rangle_{m}=\frac{1}{w\left(m\right)}\sum_{(n_1,n_2)\in\mathbb{M}(m)}\langle\widetilde{\mathbf{R}}_{\mathbb{S}}\rangle_{n_1,n_2},$$

where the set $\mathbb{M}(m)$ contains all pairs (n_1,n_2) contributing to the coarray support m, i.e.,

$$\mathbb{M}\left(m\right)=\left\{(n_1,n_2)\in\mathbb{S}^2|n_1-n_2=m\right\},\quad m\in\mathbb{D}. \tag{4}$$

Here $w(m)$ are the weight functions, given by the following definition:

Definition 6 (Weight Functions): The weight function $w(m)$ of an array $\mathbb{S}$ is defined as the number of sensor pairs that lead to coarray index m, which is exactly the cardinality of $\mathbb{M}(m)$ in (4):

$$w\left(m\right)=\left|\mathbb{M}\left(m\right)\right|,\quad m\in\mathbb{D}.$$

Notice that the weight function $w(m)$ for any linear array with N elements satisfies the following properties:

$$w\left(0\right)=N,\quad\sum_{m\in\mathbb{D}}w\left(m\right)=N^2,\quad w\left(m\right)=w\left(-m\right). \tag{5}$$

The proof of (5) follows from (4) and Definition 6.

Next, we need to estimate the true normalized DOAs $\overline{\theta}_i$ from $\widetilde{\mathbf{x}}_{\mathbb{D}}$. A variation [27] of the rank-enhanced spatial smoothing MUSIC algorithm [16] , [26] (SS MUSIC) will be used in this paper. The spatial smoothing step is avoided in [27] as follows: let the finite snapshot autocorrelation vector be $\widetilde{\mathbf{x}}_{\mathbb{D}}$. We construct a Hermitian Toeplitz matrix $\widetilde{\mathbf{R}}$ satisfying

$$\langle\widetilde{\mathbf{R}}\rangle_{n_1,n_2}=\langle\widetilde{\mathbf{x}}_{\mathbb{D}}\rangle_{n_1-n_2},$$

where $n_1,n_2\in\mathbb{U}^{+}$. The set $\mathbb{U}$ denotes the maximum contiguous ULA segment of $\mathbb{D}$. $\mathbb{U}^{+}$ is the non-negative part of $\mathbb{U}$. It was proved in [27] that the MUSIC spectrum over $\widetilde{\mathbf{R}}$ possesses the same performance as that over the spatially smoothed matrix $\widetilde{\mathbf{R}}_{ss}$, if the noise subspace is classified by the magnitudes of the eigenvalues of $\widetilde{\mathbf{R}}$.

TABLE I
SOME TERMINOLOGIES RELATED TO SPARSE ARRAYS

This paper	Alternative names
Restricted arrays [21]	Fully augmentable arrays [28]
General arrays [21]	Partially augmentable arrays [29]
Minimum redundancy arrays (MRAs)	Restricted MRAs [21]
Minimum hole arrays (MHAs)	Golomb arrays [22], Minimum-gap arrays [29]

Finally, we will review some well-known sparse array configurations, like minimum redundancy arrays (MRAs) [21] , minimum hole arrays (MHAs) [22], [23], nested arrays [16], and coprime arrays [17]. All these arrays are capable of resolving $O(N^2)$ sources provided with $O(N)$ sensors [16], [17], [21], [26], [28], and increasing the spatial resolution [16], [18]–[20], [26], [30].

MRAs [21] maximize their uniform DOF subject to a given total number of sensors. In general, MRAs may or may not be restricted [21], but in some references restricted MRAs are simply referred to as MRAs [29]. In this paper, we use the term MRAs to imply restricted MRAs. In [31], the author introduced a closed-form array geometry which yields arrays which are almost MRAs (although the author refers to these as MRAs in [31]). However, no systematic development of the properties of coarrays are included therein. MHAs [22], [23] minimize the number of holes in its coarray for a given total number of sensors, such that all the differences, except 0, occur at most once, i.e., $w(m)\in\{0,1\}$ for $m\neq 0$. MHAs are sometimes called Golomb arrays [22], or minimum-gap arrays [29]. Some common terminologies for these arrays are summarized in Table I. These arrays offer certain optimality to the array profiles but it is extremely intricate to obtain explicit expressions of the sensor locations for arbitrary number of sensors [21]–[24], [31].

Nested arrays [16] and coprime arrays [17], on the other hand, characterize their sensor locations in a closed-form, simple, and scalable fashion. For nested arrays, the sensor locations are given by

$$\begin{aligned}\mathbb{S}_{\text{nested}}=\{&1,2,...,N_1,\\&(N_1+1),2\left(N_1+1\right),...N_2\left(N_1+1\right)\},\end{aligned} \tag{6}$$

where N_1 and N_2 are positive integers. The sensor locations for coprime arrays are

$$\begin{aligned}\mathbb{S}_{\text{coprime}}=\ &\{0,M,2M,...,\left(N-1\right)M,\\&N,2N,...,\left(2M-1\right)N\},\end{aligned} \tag{7}$$

where M and N are a coprime pair of positive integers. It can be readily visualized in Fig. 3 that nested arrays are composed of two parts: dense ULA and sparse ULA. The dense ULA consists of N_1 sensors with separation $\lambda/2$ while the sparse ULA is made of N_2 sensors with separation $(N_1+1)\lambda/2$, where λ is the wavelength. On the other hand, coprime arrays comprise two ULAs. One is N sensors with spacing $M\lambda/2$ while the other is $2M-1$ sensors with spacing $N\lambda/2$. These simple expressions facilitate the design process with arbitrary number of sensors.

B. Mutual Coupling

Equation (1) assumes that the sensors do not interfere with each other. In practice, any sensor output is influenced by its neighboring elements, which is called mutual coupling. In this section, we will review mutual coupling models on sensor arrays.

Mutual coupling can be incorporated into (1) as follows:

$$\mathbf{x}_{\mathbb{S}} = \sum_{i=1}^{D} A_i \mathbf{C}\mathbf{v}_{\mathbb{S}}\left(\overline{\theta}_i\right) + \mathbf{n}_{\mathbb{S}}, \tag{8}$$

where $\mathbf{C}$ is a mutual coupling matrix that can be obtained from electromagnetics. Closed-form expressions for $\mathbf{C}$ have been investigated for decades. If the sensor array is a linear dipole array, $\mathbf{C}$ can be written as [10], [12], [32], [33]

$$\mathbf{C} = \left(Z_A + Z_L\right)\left(\mathbf{Z} + Z_L\mathbf{I}\right)^{-1}, \tag{9}$$

where Z_A and Z_L are the element/load impedance, respectively. $\langle\mathfrak{X}\rangle_{n_1,n_2}$ by

$$\begin{cases} \dfrac{\eta_0}{4\pi}\left(0.5772 + \ln\left(2\beta l\right) - \mathrm{Ci}\left(2\beta l\right) + j\mathrm{Si}\left(2\beta l\right)\right), & \text{if } n_1 = n_2, \\ \dfrac{\eta_0}{4\pi}\left(\langle\mathfrak{R}\rangle_{n_1,n_2} + j\langle\mathfrak{X}\rangle_{n_1,n_2}\right), & \text{if } n_1 \neq n_2. \end{cases}$$

Here $\eta_0 = \sqrt{\mu_0/\epsilon_0} \approx 120\pi$ is the intrinsic impedance. $\beta = 2\pi/\lambda$ is the wavenumber, where λ is the wavelength. l is the length of dipole antennas. $\mathfrak{R}$ and $\mathfrak{X}$ are

$$\begin{aligned} &\langle\mathfrak{R}\rangle_{n_1,n_2} \\ &= \sin\left(\beta l\right)\left(-\mathrm{Si}\left(u_0\right) + \mathrm{Si}\left(v_0\right) + 2\mathrm{Si}\left(u_1\right) - 2\mathrm{Si}\left(v_1\right)\right) \\ &\quad + \cos\left(\beta l\right)\left(\mathrm{Ci}\left(u_0\right) + \mathrm{Ci}\left(v_0\right) - 2\mathrm{Ci}\left(u_1\right) - 2\mathrm{Ci}\left(v_1\right)\right. \\ &\quad \left. + 2\mathrm{Ci}(\beta d_{n_1,n_2})\right) - \left(2\mathrm{Ci}(u_1) + 2\mathrm{Ci}(v_1) - 4\mathrm{Ci}(\beta d_{n_1,n_2})\right), \\ &\langle\mathfrak{X}\rangle_{n_1,n_2} \\ &= \sin\left(\beta l\right)\left(-\mathrm{Ci}\left(u_0\right) + \mathrm{Ci}\left(v_0\right) + 2\mathrm{Ci}\left(u_1\right) - 2\mathrm{Ci}\left(v_1\right)\right) \\ &\quad + \cos\left(\beta l\right)\left(-\mathrm{Si}\left(u_0\right) - \mathrm{Si}\left(v_0\right) + 2\mathrm{Si}\left(u_1\right) + 2\mathrm{Si}\left(v_1\right)\right. \\ &\quad \left. - 2\mathrm{Si}(\beta d_{n_1,n_2})\right) + \left(2\mathrm{Si}(u_1) + 2\mathrm{Si}(v_1) - 4\mathrm{Si}(\beta d_{n_1,n_2})\right), \end{aligned}$$

where $d_{n_1,n_2} = |n_1 - n_2|\lambda/2$ is the distance between sensors. The parameters u_0, v_0, u_1, and v_1 are

$$\begin{aligned} u_0 &= \beta\left(\sqrt{d_{n_1,n_2}^2 + l^2} - l\right), v_0 = \beta\left(\sqrt{d_{n_1,n_2}^2 + l^2} + l\right), \\ u_1 &= \beta\left(\sqrt{d_{n_1,n_2}^2 + 0.25l^2} - 0.5l\right), \\ v_1 &= \beta\left(\sqrt{d_{n_1,n_2}^2 + 0.25l^2} + 0.5l\right), \end{aligned}$$

$\mathrm{Si}(u)$ and $\mathrm{Ci}(u)$ are sine/cosine integrals, defined as

$$\mathrm{Si}\left(u\right) = \int_0^u \frac{\sin t}{t}\mathrm{d}t, \quad \mathrm{Ci}\left(u\right) = \int_\infty^u \frac{\cos t}{t}\mathrm{d}t.$$

Equation (9) quantifies the mutual coupling effect of linear dipole antenna arrays. Note that $\mathbf{C}$ relies on the dipole length l and the sensor element spacing d_{n_1,n_2}, which are geometric parameters.

However, (9) is too complicated to analyze. It is desirable to establish a simple mutual coupling model. The mutual coupling matrix $\mathbf{C}$ can be approximated by a B-banded symmetric Toeplitz matrix in the ULA configuration [6], [11] , [33] . It is empirically observed that the entries of $\mathbf{C}$ behave like functions of sensor separations only. In other words, we can write $\mathbf{C}$ as

$$\langle\mathbf{C}\rangle_{n_1,n_2} = \begin{cases} c_{|n_1-n_2|}, & \text{if } |n_1 - n_2| \leq B, \\ 0, & \text{otherwise}, \end{cases} \tag{10}$$

where $n_1, n_2 \in \mathbb{S}$ and coupling coefficients $c_0, c_1, ..., c_B$ satisfy $1 = c_0 > |c_1| > |c_2| > \cdots > |c_B|$. It is assumed that the magnitudes of coupling coefficients are inversely proportional to their sensor separations [6], i.e., $|c_k/c_\ell| = \ell/k$.

The mutual coupling models such as (9) and (10) are based on certain assumptions [6]–[14], [34], [35]. The actual mutual coupling matrix $\mathbf{C}$ is unknown to the user. If the mutual coupling effect is completely omitted in our estimators, the performance degrades [36]. Another approach is to estimate mutual coupling and source profiles based on particular mutual coupling models [6], [8], [11]–[14], [35]. For instance, BouDaher *et al.* considered DOA estimation with coprime arrays in the presence of mutual coupling [35]. Their algorithm jointly estimated the mutual coupling matrix $\mathbf{C}$, the source power, and the DOA under certain optimization criterion. At the expense of some extra computations, this approach estimates the true DOA satisfactorily. In principle, all of the above decoupling methods are applicable with the super nested arrays to be developed in this paper, and can only improve the performance further.

III. Mutual Coupling in Sparse Arrays: A Motivating Example

In this section, we provide an example of DOA estimation in the presence of mutual coupling for several array configurations. It will be observed that uniform DOF and weight functions of sensor arrays play a crucial role. This observation provides some insights to design sensor arrays that reduce the mutual coupling effect.

In Fig. 4, we evaluate the performance of ULAs, MRAs [21], nested arrays [16], and coprime arrays [17], [26] in the presence of mutual coupling. The number of sensors is 6 for each array. Then, the sensor locations are given by (6) with $N_1 = N_2 = 3$ for nested arrays and (7) with $M = 2$ and $N = 3$ for coprime arrays. The sensor locations are listed on the first row of Fig. 4. The number of sources $D = 4$ and the DOA profiles are $\overline{\theta}_1 = 0, \overline{\theta}_2 = 0.1, \overline{\theta}_3 = 0.2$, and $\overline{\theta}_4 = 0.3$. The SNR is 0 dB and the number of snapshots K is 1000. The mutual coupling matrix $\mathbf{C}$ is based on (10), where $c_0 = 1, c_1 = 0.5e^{j\pi/4}, c_2 = 0.5e^{j0.7\pi}/2, c_3 = 0.5e^{j0.7\pi}/3$, and $B = 3$. The measurement with mutual coupling can be expressed as in (8). The DOAs are estimated from the measurement vectors without any decoupling algorithms [6], [8] , [11]–[14], [35].

The second row of Fig. 4 shows weight functions of different array geometries. The coarray of ULA has consecutive integers from -5 to 5, the coarray of MRA ranges from -13 to 13, the nested array owns coarray aperture from -11 to 11, and the coprime array has the maximum contiguous ULA section in its coarray domain from -7 to 7. Then, the uniform DOF, as defined in Definition 3, for ULA, MRA, the nested array, the coprime array are 11, 27, 23, and 15, respectively. Hence, the maximum number of detectable sources for ULA,

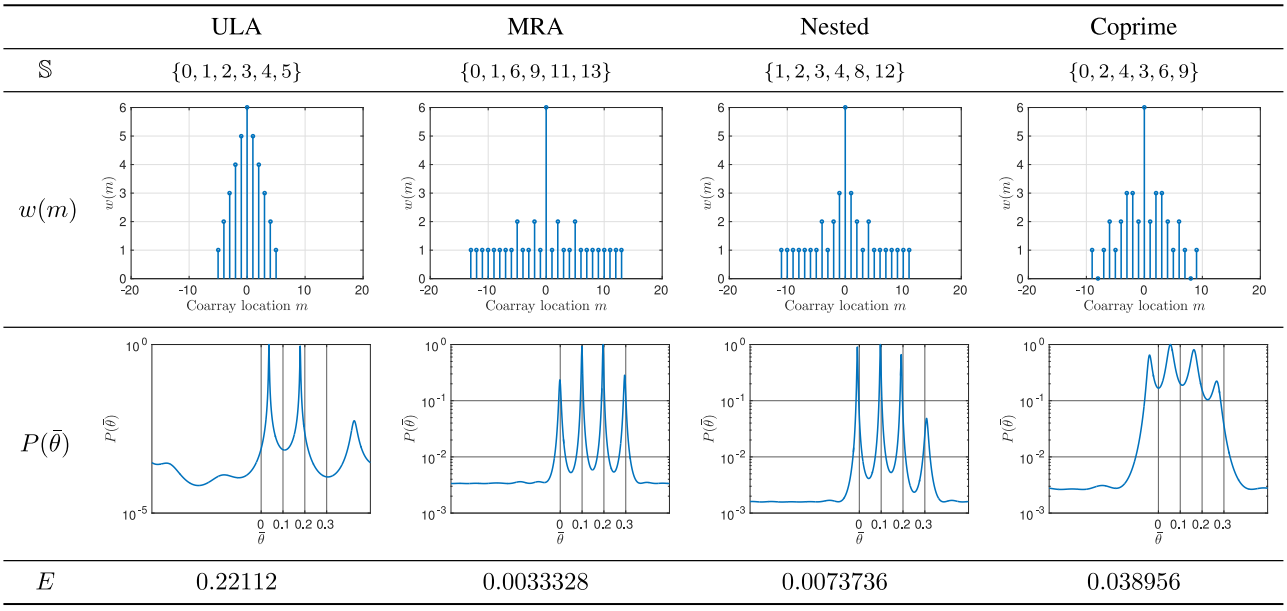

Fig. 4. Comparison among ULAs, MRAs, nested arrays, coprime arrays and their MUSIC spectra $P(\overline{\theta})$ in the presence of mutual coupling. It can be observed that higher uniform DOF and smaller weight functions $w(1), w(2), w(3)$ tend to decrease the RMSE.

MRA, nested array, and coprime array is 5, 13, 11, and 7, respectively [16], [26]. The MUSIC algorithm is performed for ULA while the coarray MUSIC (SS MUSIC) is used in all the sparse arrays. In addition, the weight functions $w(m)$ also exhibit different distributions for different arrays. If we consider $w(1)$ among all these arrays, we obtain $w(1) = 5, 1, 3, 2$ for ULA, MRA, nested arrays, and coprime arrays, respectively. When $w(1)$ becomes smaller, there are fewer sensor pairs with separation 1 so, qualitatively, we obtain a sparser array configuration.

The associated MUSIC spectra $P(\overline{\theta})$ and the root-mean-squared error (RMSE), are shown on the third row and the fourth row of Fig. 4, respectively. The RMSE (E) is defined as

$$E = \sqrt{\frac{1}{D}\sum_{i=1}^{D}\left(\widehat{\overline{\theta}}_i - \overline{\theta}_i\right)^2}, \tag{11}$$

where $\widehat{\overline{\theta}}_i$ denotes the estimated normalized DOA of the ith source, according to the root MUSIC algorithm, and $\overline{\theta}_i$ is the true normalized DOA. It can be observed that ULA fails to identify four sources accurately in this example, while MRA has the best estimation performance. In nested arrays and coprime arrays, four peaks can be seen but they have more estimation error. These spectra conclude the estimation performance: MRA is the best one, followed by nested arrays and then coprime arrays. ULA has the worst performance. In the example of Section VI (Fig. 8) we will see that super nested arrays can achieve significantly smaller error than MRAs in the presence of mutual coupling.

Fig. 4 provides some insightful *qualitative* statements. First, as the uniform DOF increases, the corresponding RMSE decreases. The size of this virtual ULA, or equivalently the uniform DOF, is 27 for MRA, 23 for the nested array, 15 for the coprime array, and 11 for ULA. This explains why the RMSE is the least for the MRA, followed by the nested array, coprime array and lastly the ULA.

Second, the RMSE also tends to decrease as the weight functions $w(1), w(2)$, and $w(3)$ decrease. However, this qualitative argument cannot be concluded from Fig. 4 directly, since these examples have different uniform DOFs and weight functions. For a meaningful comparison, let us look at the nested array and the super nested array. As presented in Section V, the uniform DOF of the super nested array is identical to that of the nested array while the weight functions $w(1), w(2)$, and $w(3)$ of the super nested array are smaller than those of the nested array. It is observed from Figs. 8 to 11 that the RMSE of the super nested array are less than those of the nested array. This phenomenon can be elaborated as follows: Decreasing these weights reduces the number of sensor pairs with significant mutual coupling. Less mutual coupling implies the mutual coupling matrix $\mathbf{C}$ is closer to the identity matrix, which makes the RMSE likely to decrease.

Based on these observations, the MRA seems to be the best array with minimum mutual coupling since it owns the maximum DOF as well as the smallest $w(1), w(2)$, and $w(3)$. However, it is quite intricate to determine the MRA configuration. First, the sensor locations of MRA can only be found using combinatorial search or table lookup [21], [31]. This is neither scalable nor practical if our design budget is a large number of sensors, say, 100 physical sensors. On the other hand, if our design budget is a fixed array aperture, which exists in applications such as airplane, submarine, or mobile devices, MRA might not be optimal. For instance, provided the available space being $11d$, we cannot use the MRA in Fig. 4 since its total aperture is $13d$. If we apply MRA with 5 sensors, we obtain $\mathbb{S} = \{0, 1, 4, 7, 9\}$ but

the maximum number of distinguishable sources decreases to 9. The space is not fully utilized.

Like MRA, nested and coprime arrays also have $O(N^2)$ uniform DOF given $O(N)$ sensors but they have closed-form expressions for sensor locations for any N. Even though their uniform DOF are less than those of MRA, they offer simple design equations. These equations admit simple calculations and regular array geometries. In some situations, the nested arrays can be superior to MRAs. For example, under the constraint that the available aperture is $11d$, the nested array with $N_1 = 3$ and $N_2 = 3$ is an acceptable design, and it resolves 11 sources. The MRA with 5 sensors can only resolve 9 sources.

According to Fig. 4, it is tempting to conclude that nested arrays are superior to coprime arrays but this is not always true. The estimation performance depends heavily on the mutual coupling coefficients. If mutual coupling is negligible, the performance is governed by the uniform DOF, implying nested arrays are superior [16], [17]. However, as mutual coupling becomes severe, the performance of nested arrays worsens much more than that of coprime arrays, as we shall see in Section VII of the companion paper [37] later. This is because nested arrays contain a dense ULA part, while coprime arrays have only two pairs of sensors with separation one [17] .

Presented with these issues, we are motivated to find a sparse array configuration that satisfies the following three criteria:

1) The sensor locations should be describable using *simple rules or closed forms* as in the case of nested and coprime arrays.
2) The coarray of the sparse array should have a *large contiguous ULA section*. In fact we will aim for sparse arrays whose coarrays are ULAs (i.e., hole free) of the same size as coarrays of nested arrays.
3) The weight functions $w(1), w(2)$, and $w(3)$ have to be *small*. It is preferable to achieve $w(1) \leq w_{\text{coprime}}(1) = 2$, so that mutual coupling can be mitigated in the new array configuration.

IV. Second-Order Super Nested Arrays

In this section, we develop second-order super nested arrays. For fixed number of sensors, these have the same physical aperture and the same difference coarray enjoyed by nested arrays (in particular there are no holes in coarray). But they have reduced mutual coupling because of smaller values of the crucial weights $w(1), w(2)$, and $w(3)$.

Nested arrays are parametrized by integers N_1 and N_2, which denote the number of sensors in the dense ULA part and the sparse ULA part, respectively. To alleviate mutual coupling, we need to remove some sensors in the first layer (dense ULA part) and relocate them appropriately, keeping in mind the three criteria at the end of the preceding section. Note that there are many rearrangements to nested arrays that satisfy our design criteria. We will show that the following array geometry is a valid solution:

Definition 7 (Second-Order Super Nested Arrays): Assume N_1 and N_2 are integers satisfying $N_1 \geq 4$ and $N_2 \geq 3$. Second-order super nested arrays are specified by the integer set $\mathbb{S}^{(2)}$, defined by

$$\mathbb{S}^{(2)} = \mathbb{X}_1^{(2)} \cup \mathbb{Y}_1^{(2)} \cup \mathbb{X}_2^{(2)} \cup \mathbb{Y}_2^{(2)} \cup \mathbb{Z}_1^{(2)} \cup \mathbb{Z}_2^{(2)},$$

where

$$\begin{aligned}
\mathbb{X}_1^{(2)} &= \{1 + 2\ell | 0 \leq \ell \leq A_1\}, \\
\mathbb{Y}_1^{(2)} &= \{(N_1 + 1) - (1 + 2\ell) | 0 \leq \ell \leq B_1\}, \\
\mathbb{X}_2^{(2)} &= \{(N_1 + 1) + (2 + 2\ell) | 0 \leq \ell \leq A_2\}, \\
\mathbb{Y}_2^{(2)} &= \{2(N_1 + 1) - (2 + 2\ell) | 0 \leq \ell \leq B_2\}, \\
\mathbb{Z}_1^{(2)} &= \{\ell(N_1 + 1) | 2 \leq \ell \leq N_2\}, \\
\mathbb{Z}_2^{(2)} &= \{N_2(N_1 + 1) - 1\}.
\end{aligned}$$

The parameters A_1, B_1, A_2, and B_2 are defined as

$$(A_1, B_1, A_2, B_2) = \begin{cases} (r, r-1, r-1, r-2), & \text{if } N_1 = 4r, \\ (r, r-1, r-1, r-1), & \text{if } N_1 = 4r+1, \\ (r+1, r-1, r, r-2), & \text{if } N_1 = 4r+2, \\ (r, r, r, r-1), & \text{if } N_1 = 4r+3, \end{cases}$$

where r is an integer.

A MATLAB code for generating super nested arrays can be found in [25]. The function `super_nested.m` takes N_1 and N_2 as inputs and returns the set $\mathbb{S}^{(2)}$. (The parameter Q should be set to 2; higher Q produces higher order super nested arrays described in the companion paper [37]). In addition, `interactive_interface.m` offers an interactive panel where users can design their array configurations over 2D representations and visualize the associated weight functions easily.

Note that Definition 7 is applicable to $N_1 \geq 4$. In particular, if $N_1 = 4$ or 6, then the sets $\mathbb{X}_1^{(2)}$, $\mathbb{Y}_1^{(2)}$, and $\mathbb{X}_2^{(2)}$ are non-empty but the set $\mathbb{Y}_2^{(2)}$ becomes the empty set, since the parameter $B_2 = -1$. Otherwise, if N_1 is 5, or greater than 6, the sets $\mathbb{X}_1^{(2)}, \mathbb{Y}_1^{(2)}, \mathbb{X}_2^{(2)}$, and $\mathbb{Y}_2^{(2)}$ are non-empty.

As an example, let us consider second-order super nested arrays with various combinations of N_1 and N_2. In Fig. 5(a), $N_1 = 10$ and $N_2 = 4$ while in Fig. 5(b), $N_1 = N_2 = 7$. It can be observed that there are $N_1 + N_2 = 14$ sensors in each configuration. The total aperture becomes 43 and 55 in parts (a) and (b), respectively. The difference coarray for (a) and (b) comprises consecutive integers from -43 to 43, and -55 to 55, respectively.

Next, the relationship between nested arrays and second-order super nested arrays is elaborated in Fig. 6(a) and (b) for $N_1 = N_2 = 13$. These *linear arrays* are shown in terms of their 2D representations, as defined in Fig. 1. The dashed rectangles mark the support of dense ULA, sparse ULA, $\mathbb{X}_1^{(2)}, \mathbb{Y}_1^{(2)}, \mathbb{X}_2^{(2)}, \mathbb{Y}_2^{(2)}, \mathbb{Z}_1^{(2)}$, and $\mathbb{Z}_2^{(2)}$, respectively. It can be seen from Fig. 6(a) and (b) that second-order super nested arrays modify nested arrays in two ways. First, the sensors in the dense ULA part of nested arrays are broken into four ULA sections $\mathbb{X}_1^{(2)}, \mathbb{Y}_1^{(2)}, \mathbb{X}_2^{(2)}$, and $\mathbb{Y}_2^{(2)}$ in second-order super nested arrays. Each of them possesses inter-element spacing 2. In addition, the sensor at location $N_1 + 1$ is moved to $N_2(N_1 + 1) - 1$. The weight function $w(1)$ for nested arrays and second-order

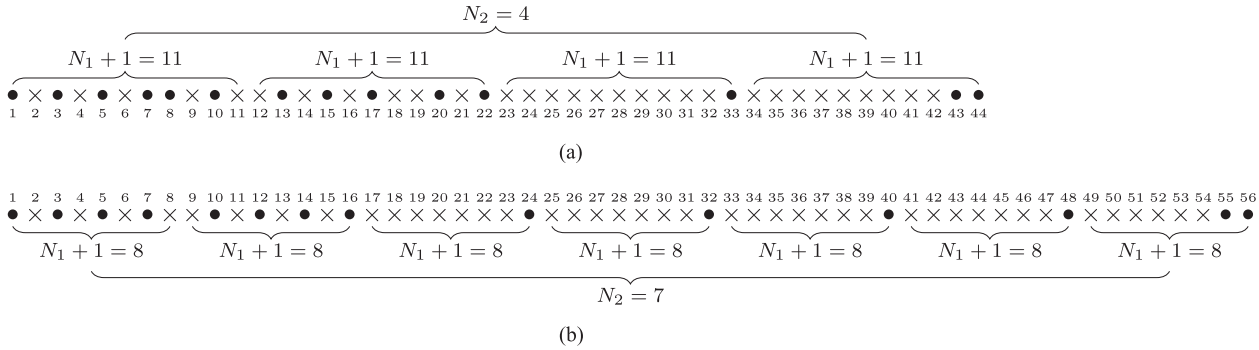

Fig. 5. 1D representations of second-order super nested arrays with (a) $N_1 = 10, N_2 = 4$, and (b) $N_1 = N_2 = 7$. Bullets stand for physical sensors and crosses represent empty space. Both configurations consist of 14 physical sensors but (b) leads to larger total aperture and a sparser pattern. It will be proved that the uniform DOF of (a) and (b) are $2N_2(N_1 + 1) - 1$, which are 87 and 111, respectively.

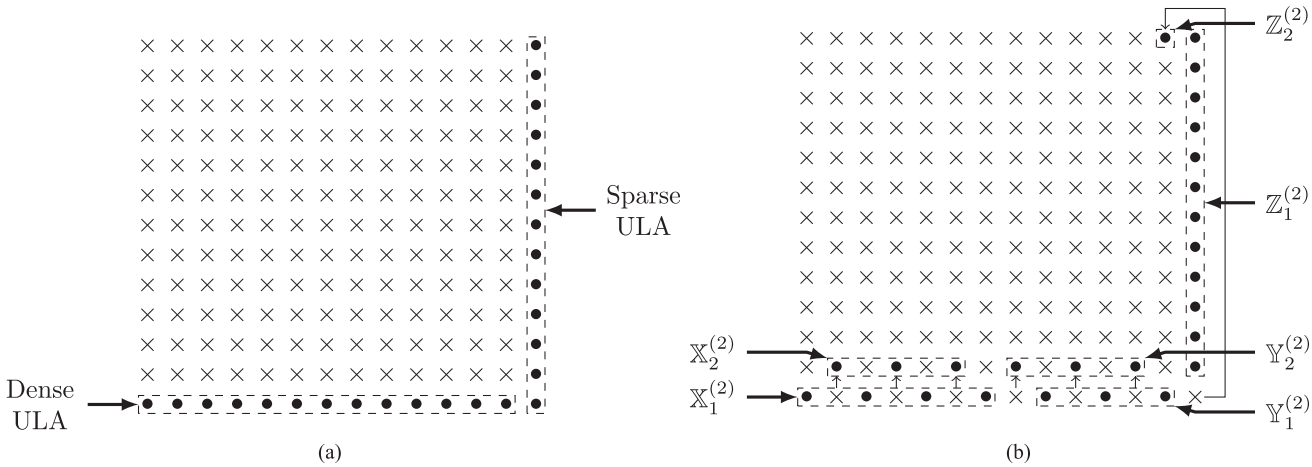

Fig. 6. 2D representations of (a) the parent nested array, and (b) the corresponding second-order super nested array, $\mathbb{S}^{(2)}$, where $N_1 = N_2 = 13$. Bullets denote sensor locations while crosses indicate empty locations. Thin arrows illustrate how sensors migrate from nested arrays to second-order super nested arrays. The dense ULA in nested arrays is split into four sets: $\mathbb{X}_1^{(2)}$, $\mathbb{Y}_1^{(2)}$, $\mathbb{X}_2^{(2)}$, and $\mathbb{Y}_2^{(2)}$ in second-order super nested arrays. The sensor located at $N_1 + 1$, belonging to the sparse ULA of nested arrays, is moved to location $N_2(N_1 + 1) - 1$ in second-order super nested arrays.

	ULA	MRA	Nested	Coprime	Second-order super nested	Third-order super nested
$w(m)$	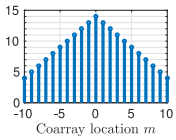	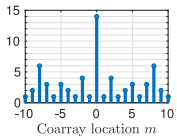	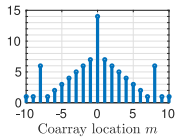	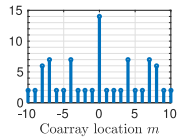	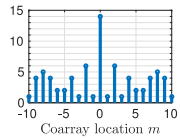	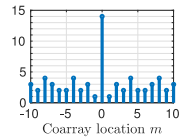
$\mathbf{C}$	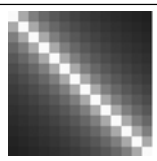	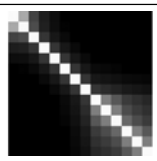	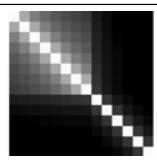	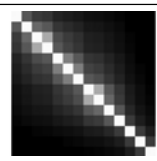	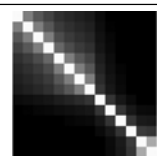	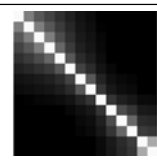
L	0.44132	0.18243	0.33327	0.21426	0.20295	0.18203

Fig. 7. Comparison among ULA, nested array, coprime array, second-order super nested array, and third-order super nested array in the presence of mutual coupling. The coupling leakage L is defined as $\| \mathbf{C} - \mathrm{diag}(\mathbf{C}) \|_F / \| \mathbf{C} \|_F$, where $[\mathrm{diag}(\mathbf{C})]_{i,j} = [\mathbf{C}]_{i,j}\delta_{i,j}$.

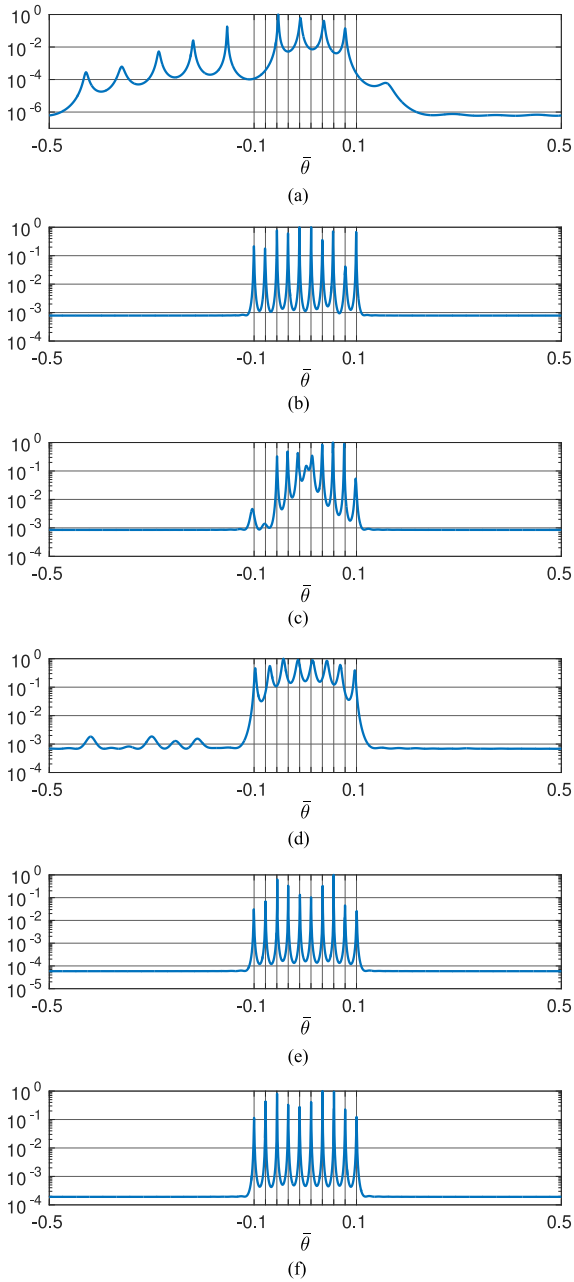

Fig. 8. The MUSIC spectra $P(\bar{\theta})$ for ULA, MRA, nested arrays, coprime arrays, second-order super nested arrays, and third-order super nested arrays when $D = 10$ sources are located at $\bar{\theta}_i = -0.1 + 0.2(i-1)/9, i = 1, 2, ..., 10$, as depicted by ticks and vertical lines. The SNR is 0 dB while the number of snapshots is $K = 500$. Note that the number of sources 10 is less than the number of sensors 14. The mutual coupling is based on (10) with $c_1 = 0.3e^{j\pi/3}$, $B = 100$, and $c_\ell = c_1 e^{-j(\ell-1)\pi/8}/\ell$ for $2 \le \ell \le B$. (a) ULA, $D = 10, E = 0.17445$. (b) MRA, $D = 10, E = 0.00060242$. (c) Nested array, $D = 10, E = 0.01216$. (d) Coprime array, $D = 10, E = 0.12509$. (e) Second-order super nested, $D = 10, E = 0.00042112$. (f) Third-order super nested, $D = 10, E = 0.00023647$.

super nested arrays are 13 and 1, respectively. Second-order super nested arrays significantly decrease the number of sensor pairs with separation 1. As a result, second-order super nested arrays are qualitatively sparser than nested arrays and mutual coupling effect could alleviate.

In the following development, as a shorthand notation, the addition between a set and a scalar is defined as

$$\mathbb{A} \pm c = \{a \pm c | \forall a \in \mathbb{A}\}.$$

Provided with two sets $\mathbb{A}$ and $\mathbb{B}$, the difference set between $\mathbb{A}$ and $\mathbb{B}$ is given by

$$\text{diff}(\mathbb{A}, \mathbb{B}) = \{a - b | a \in \mathbb{A}, b \in \mathbb{B}\}.$$

It can be seen that $\text{diff}(\mathbb{A}, \mathbb{B})$ does not necessarily equal to $\text{diff}(\mathbb{B}, \mathbb{A})$. Next, some simple properties of second-order super nested arrays are proved. More advanced properties pertaining to the difference coarray will be proved in Section V.

Lemma 1 (Relation to the Dense ULA of the Parent Nested Array): Let $\mathbb{X}_1^{(2)}, \mathbb{Y}_1^{(2)}, \mathbb{X}_2^{(2)}$, and $\mathbb{Y}_2^{(2)}$ be given in Definition 7. Then

$$\mathbb{X}_1^{(2)} \cup \mathbb{Y}_1^{(2)} \cup \left(\mathbb{X}_2^{(2)} - (N_1+1)\right) \cup \left(\mathbb{Y}_2^{(2)} - (N_1+1)\right) = \{1, 2, ..., N_1\}.$$

Proof: According to Definition 7, $\mathbb{X}_1^{(2)}$ collects all the odd numbers from 1 to $1 + 2A_1$ while $\mathbb{X}_2^{(2)} - (N_1+1)$ includes all the even numbers ranging from 2 to $2 + 2A_2$. As a result, we have

$$\mathbb{X}_1^{(2)} \cup \left(\mathbb{X}_2^{(2)} - (N_1+1)\right) \supseteq \{1, 2, ..., \min(1+2A_1, 2+2A_2) + 1\}. \quad (12)$$

Furthermore, it can be shown that $|\max(\mathbb{X}_1^{(2)}) - \max(\mathbb{X}_2^{(2)} - (N_1+1))| = |(1+2A_1) - (2+2A_2)| = 1$. Therefore, we can replace the inclusion $(\supseteq)$ in (12) with equality $(=)$ and obtain

$$\begin{aligned}
&\mathbb{X}_1^{(2)} \cup \left(\mathbb{X}_2^{(2)} - (N_1+1)\right) \\
&\quad = \{1, 2, ..., \min(1+2A_1, 2+2A_2) + 1\} \\
&\quad = \begin{cases} \{1, 2, ..., 2r+1\}, & \text{if } N_1 = 4r, \\ \{1, 2, ..., 2r+1\}, & \text{if } N_1 = 4r+1, \\ \{1, 2, ..., 2r+3\}, & \text{if } N_1 = 4r+2, \\ \{1, 2, ..., 2r+2\}, & \text{if } N_1 = 4r+3. \end{cases}
\end{aligned}$$

Similarly, $\mathbb{Y}_1^{(2)}$ and $\mathbb{Y}_2^{(2)} - (N_1+1)$ give

$$\begin{aligned}
&\mathbb{Y}_1^{(2)} \cup \left(\mathbb{Y}_2^{(2)} - (N_1+1)\right) \\
&\quad = \{\max(N_1 - 2B_1, N_1 - 1 - 2B_2) - 1, ..., N_1\} \\
&\quad = \begin{cases} \{2r+2, ..., N_1\}, & \text{if } N_1 = 4r, \\ \{2r+2, ..., N_1\}, & \text{if } N_1 = 4r+1, \\ \{2r+4, ..., N_1\}, & \text{if } N_1 = 4r+2, \\ \{2r+3, ..., N_1\}, & \text{if } N_1 = 4r+3. \end{cases}
\end{aligned}$$

Whichever N_1 is, the union of these four sets covers all the integers from 1 to N_1. ■

Lemma 2 (Total Number of Sensors): The number of elements in $\mathbb{S}^{(2)}$ is $N_1 + N_2$.

Proof: Firstly, $\mathbb{X}_1^{(2)}, \mathbb{Y}_1^{(2)}, \mathbb{X}_2^{(2)}, \mathbb{Y}_2^{(2)}, \mathbb{Z}_1^{(2)}$, and $\mathbb{Z}_2^{(2)}$ are disjoint, which can be easily checked from Definition 7. Thus, the

cardinality of $\mathbb{S}^{(2)}$ is the same as the sum of the cardinality of the individual set. We obtain

$$\begin{aligned}|\mathbb{S}^{(2)}| &= \left(\sum_{q=1}^{2}|\mathbb{X}_q^{(2)}|+|\mathbb{Y}_q^{(2)}|\right)+|\mathbb{Z}_1^{(2)}|+|\mathbb{Z}_2^{(2)}|\\ &= \left(\sum_{q=1}^{2}(A_q+1)_+ +(B_q+1)_+\right)+(N_2-1)+1\\ &= N_1+N_2,\end{aligned}$$

where $(x)_+ = \max(x,0)$ denotes the non-negative part of x. Therefore, there are N_1+N_2 sensor in second-order super nested arrays. ■

V. Coarray of Second-Order Super Nested Arrays

In this section, we will show that super nested arrays are restricted arrays, that is, the coarray does not have holes. This property enables us to apply algorithms such as MUSIC in the coarray domain conveniently, as in the case of nested arrays and MRAs. We will also derive the expressions for the first few weight functions $w(m)$ of the super nested array.

Theorem 1: Second-order super nested arrays are restricted arrays, i.e., they have hole-free difference coarrays.

Proof: The statement that a second-order super nested array is a restricted array, is equivalent to the following argument: For every m ranging from $-(N_2(N_1+1)-1)$ to $N_2(N_1+1)-1$, there exists at least one pair of physical sensors with sensor separation m. Nevertheless, we do not need to check all possible m's according to the following properties:

1) If m is in the coarray, $-m$ also belongs to the same coarray.
2) $m=0$ is included in any coarray.

Therefore, it suffices to check that for $1\le m\le N_2(N_1+1)-1$, we can identify at least one pair $(n_1,n_2)\in(\mathbb{S}^{(2)})^2$ such that $n_1-n_2=m$.

If $m=1$, the sensors on $N_2(N_1+1)-1\in\mathbb{Z}_2^{(2)}$ and $N_2(N_1+1)\in\mathbb{Z}_1^{(2)}$ contribute to $w(1)$.

When $2\le m\le N_1$, we turn to evaluate the following sets:

$$\begin{aligned}&\text{diff}\left(\{2(N_1+1)\},\mathbb{X}_2^{(2)}\cup\mathbb{Y}_2^{(2)}\right)\\ &\quad=\{N_1-1-2\ell|0\le\ell\le A_2\}\\ &\qquad\cup\{2+2\ell|0\le\ell\le B_2\},\\ &\text{diff}\left(\{N_1+3\},\mathbb{X}_1^{(2)}\cup\mathbb{Y}_1^{(2)}\right)\\ &\quad=\{N_1+2-2\ell|0\le\ell\le A_1\}\\ &\qquad\cup\{3+2\ell|0\le\ell\le B_1\}.\end{aligned}$$

It is clear that these sets are contained in the difference coarray since $2(N_1+1)\in\mathbb{Z}_1^{(2)}$ and $N_1+3\in\mathbb{X}_2^{(2)}$. Note that the set $\{2+2\ell|0\le\ell\le B_2\}$ includes all the even numbers starting from 2 to $2+2B_2$ while $\{3+2\ell|0\le\ell\le B_1\}$ collects all the odd numbers from 3 to $3+2B_1$. This observation is summarized into

$$\begin{aligned}\mathbb{P}_1&=\{m|2\le m\le\min(3+2B_1,2+2B_2)+1\}\\ &\subseteq\{2+2\ell|0\le\ell\le B_2\}\cup\{3+2\ell|0\le\ell\le B_1\},\end{aligned}$$

which indicates that the contiguous integers from 2 to $\min(3+2B_1,2+2B_2)+1$, denoted by $\mathbb{P}_1$, are contained in the coarray of second-order super nested arrays. A similar result for $\{N_1-1-2\ell|0\le\ell\le A_2\}$ and $\{N_1+2-2\ell|0\le\ell\le A_1\}$ is given by the set $\mathbb{P}_2$:

$$\begin{aligned}\mathbb{P}_2&=\{m|\max(N_1+2-2A_1,N_1-1-2A_2)-1\le m\le N_1\}\\ &\subseteq\{N_1-1-2\ell|0\le\ell\le A_2\}\cup\{N_1+2-2\ell|0\le\ell\le A_1\}.\end{aligned}$$

It can be verified in Table II that $\mathbb{P}_1\cup\mathbb{P}_2$ contains all the differences within $2\le m\le N_1$, except for $N_1=4r,4r+2$, and $4r+3$. In the case of $N_1=4r$, the coarray index $2r$ can be found in the pair of sensors on $1\in\mathbb{X}_1^{(2)}$ and $1+2A_1\in\mathbb{X}_1^{(2)}$. When $N_1=4r+2$, the pair of sensors on $(N_1+1)+2\in\mathbb{X}_2^{(2)}$ and $(N_1+1)+(2+2A_2)\in\mathbb{X}_2^{(2)}$ leads to coarray index $2r$. If $N_1=4r+3$, the differences $2r+2$ and $2r+3$ are exactly N_1-1-2A_2 and $3+2B_1$, respectively, as shown in Table II. Hence, $2\le m\le N_1$ is included in the difference coarray.

TABLE II
Ranges of $\mathbb{P}_1$ and $\mathbb{P}_2$

N_1	$4r$	$4r+1$	$4r+2$	$4r+3$
$3+2B_1$	$2r+1$	$2r+1$	$2r+1$	$2r+3$
$2+2B_2$	$2r-2$	$2r$	$2r-2$	$2r$
$\max(\mathbb{P}_1)$	$2r-1$	$2r+1$	$2r-1$	$2r+1$
N_1+2-2A_1	$2r+2$	$2r+3$	$2r+2$	$2r+5$
N_1-1-2A_2	$2r+1$	$2r+2$	$2r+1$	$2r+2$
$\min(\mathbb{P}_2)$	$2r+1$	$2r+2$	$2r+1$	$2r+4$
Holes in $\mathbb{P}_1\cup\mathbb{P}_2$	$2r$	–	$2r$	$2r+2, 2r+3$

For the coarray index $q(N_1+1)\le m\le(q+1)(N_1+1)$, where $1\le q\le N_2-2$, we consider the differences

$$\begin{aligned}&\text{diff}\left(\{(q+1)(N_1+1)\},\mathbb{X}_1^{(2)}\cup\mathbb{Y}_1^{(2)}\right)\\ &\quad=\text{diff}\left(\{N_1+1\},\mathbb{X}_1^{(2)}\cup\mathbb{Y}_1^{(2)}\right)+q(N_1+1),\\ &\text{diff}\left(\{(q+2)(N_1+1)\},\mathbb{X}_2^{(2)}\cup\mathbb{Y}_2^{(2)}\right)\\ &\quad=\text{diff}\left(\{N_1+1\},\left(\mathbb{X}_2^{(2)}-(N_1+1)\right)\right.\\ &\qquad\left.\cup\left(\mathbb{Y}_2^{(2)}-(N_1+1)\right)\right)+q(N_1+1),\end{aligned}$$

According to Lemma 1, the union of $\text{diff}(\{N_1+1\},\mathbb{X}_1^{(2)}\cup\mathbb{Y}_1^{(2)})$ and $\text{diff}(\{N_1+1\},(\mathbb{X}_2^{(2)}-(N_1+1))\cup(\mathbb{Y}_2^{(2)}-(N_1+1)))$ covers all the consecutive integers from 1 to N_1. In other words, the coarray index $q(N_1+1)<m<(q+1)(N_1+1)$ can be found in the difference sets among $\mathbb{X}_1^{(2)},\mathbb{Y}_1^{(2)},\mathbb{X}_2^{(2)},\mathbb{Y}_2^{(2)}$, and $\mathbb{Z}_1^{(2)}$. It is obvious that the differences $q(N_1+1)$ are contained in the self-difference of $\mathbb{Z}_1^{(2)}$.

The last part of the proof considers $(N_2-1)(N_1+1)\le m\le N_2(N_1+1)-1$. In this case, we take the following four

TABLE III
RANGES OF $\mathbb{X}_1^{(2)} \cup (\mathbb{X}_1^{(2)}+1)$ AND $\mathbb{Y}_1^{(2)} \cup (\mathbb{Y}_1^{(2)}+1)$

N_1	$4r$	$4r+1$	$4r+2$	$4r+3$
$\max(\mathbb{X}_1^{(2)} \cup (\mathbb{X}_1^{(2)}+1)) = 2+2A_1$	$2r+2$	$2r+2$	$2r+4$	$2r+2$
$\min(\mathbb{Y}_1^{(2)} \cup (\mathbb{Y}_1^{(2)}+1)) = (N_1+1)-(1+2B_1)$	$2r+2$	$2r+3$	$2r+4$	$2r+3$

sets: $\text{diff}(\{N_2(N_1+1)\}, \mathbb{X}_1^{(2)})$, $\text{diff}(\{N_2(N_1+1)\}, \mathbb{Y}_1^{(2)})$, and

$$\text{diff}\left(\{N_2(N_1+1)-1\}, \mathbb{X}_1^{(2)}\right) = \text{diff}\left(\{N_2(N_1+1)\}, \mathbb{X}_1^{(2)}+1\right),$$

$$\text{diff}\left(\{N_2(N_1+1)-1\}, \mathbb{Y}_1^{(2)}\right) = \text{diff}\left(\{N_2(N_1+1)\}, \mathbb{Y}_1^{(2)}+1\right).$$

To prove these difference sets cover $(N_2-1)(N_1+1) \le m \le N_2(N_1+1)-1$, it suffices to show that $\mathbb{X}_1^{(2)} \cup \mathbb{Y}_1^{(2)} \cup (\mathbb{X}_1^{(2)}+1) \cup (\mathbb{Y}_1^{(2)}+1)$ contains contiguous integers from 1 to N_1+1. Note that $\mathbb{X}_1^{(2)} \cup (\mathbb{X}_1^{(2)}+1)$ is $\{1, ..., 2+2A_1\}$ and $\mathbb{Y}_1^{(2)} \cup (\mathbb{Y}_1^{(2)}+1)$ is $\{(N_1+1)-(1+2B_1), ..., N_1+1\}$. Table III shows the maximum element in $\mathbb{X}_1^{(2)} \cup (\mathbb{X}_1^{(2)}+1)$ and the minimum element in $\mathbb{Y}_1^{(2)} \cup (\mathbb{Y}_1^{(2)}+1)$. It is evident that there are no holes in $\mathbb{X}_1^{(2)} \cup \mathbb{Y}_1^{(2)} \cup (\mathbb{X}_1^{(2)}+1) \cup (\mathbb{Y}_1^{(2)}+1)$. This completes the proof. ■

Corollary 1: Second-order super nested arrays have the same coarray as their parent nested arrays.

Proof: According Definition 7, second-order super nested arrays share the same boundary points, located at 1 and $N_2(N_1+1)$, as their parent nested arrays. In addition, both of them are restricted arrays (Theorem 1). Therefore, they possess the same coarray. ■

Theorem 2: Let $\mathbb{S}^{(2)}$ be a second-order super nested array with $N_1 \ge 4, N_2 \ge 3$. Its weight function $w(m)$ at $m = 1, 2, 3$ is

$$w(1) = \begin{cases} 2, & \text{if } N_1 \text{ is even,} \\ 1, & \text{if } N_1 \text{ is odd,} \end{cases}$$

$$w(2) = \begin{cases} N_1-3, & \text{if } N_1 \text{ is even,} \\ N_1-1, & \text{if } N_1 \text{ is odd,} \end{cases}$$

$$w(3) = \begin{cases} 3, & \text{if } N_1 = 4, 6, \\ 4, & \text{if } N_1 \text{ is even, } N_1 \ge 8, \\ 1, & \text{if } N_1 \text{ is odd.} \end{cases}$$

For comparison, the first three weight functions for nested arrays [16] and coprime arrays [17], [26] are

$$\text{Nested}: \; w(1) = N_1, w(2) = N_1-1, w(3) = N_1-2, \tag{13}$$

$$\text{Coprime}: \; w(1) = w(2) = w(3) = 2, \tag{14}$$

where N_1, N_2 for nested arrays and M, N for coprime arrays are sufficiently large. As a result, $w(1)$ and $w(3)$ for second-order super nested arrays are notably smaller than those for their parent nested array, and comparable to those for coprime arrays. The proof of Theorem 2 is as follows:

Proof: First, we analyze the structure of the positive part of the difference coarray. It is known that, if the array configuration $\mathbb{S} = \mathbb{A} \cup \mathbb{B}$, then the difference coarray $\mathbb{D}$ can be divided into *self differences*, like $\text{diff}(\mathbb{A}, \mathbb{A})$, $\text{diff}(\mathbb{B}, \mathbb{B})$, and *cross differences*, such as $\text{diff}(\mathbb{A}, \mathbb{B})$, $\text{diff}(\mathbb{B}, \mathbb{A})$ [17]. We will use this approach to prove Theorem 2.

The self differences are discussed as follows: According to Definition 7, since $\mathbb{X}_1^{(2)}, \mathbb{Y}_1^{(2)}, \mathbb{X}_2^{(2)}$, and $\mathbb{Y}_2^{(2)}$ are ULAs with separation 2, their self differences contain $0, \pm 2, \pm 4, \pm 6$, and so on. We obtain

$$(A_1)_+ + (B_1)_+ + (A_2)_+ + (B_2)_+ \tag{15}$$

pairs of sensors with separation 2, where $(x)_+ = \max(x, 0)$ is the positive part of a real number x. Next, it can be shown that the self differences of $\mathbb{Z}_1^{(2)}$ include $0, \pm(N_1+1), \pm 2(N_1+1), \pm 3(N_1+1)$, up to $\pm(N_2-2)(N_1+1)$. Since $N_1 \ge 4$, the self differences of $\mathbb{Z}_1^{(2)}$ do not contain 1, 2, and 3. The self difference of $\mathbb{Z}_2^{(2)}$ is exactly zero because there is only one element in $\mathbb{Z}_2^{(2)}$.

For the cross differences, it suffices to consider the sets of interest: $\text{diff}(\mathbb{Y}_1^{(2)}, \mathbb{X}_1^{(2)})$, $\text{diff}(\mathbb{X}_2^{(2)}, \mathbb{Y}_1^{(2)})$, $\text{diff}(\mathbb{Y}_2^{(2)}, \mathbb{X}_2^{(2)})$, $\text{diff}(\{2(N_1+1)\}, \mathbb{Y}_2^{(2)})$, and $\text{diff}(\{N_2(N_1+1)\}, \mathbb{Z}_2^{(2)})$, since the remaining choices of cross differences, like $\text{diff}(\mathbb{X}_2^{(2)}, \mathbb{X}_1^{(2)})$, $\text{diff}(\mathbb{Z}_1^{(2)}, \mathbb{X}_1^{(2)})$, and so on, do not include 1, 2, and 3. Evaluating the minimum elements of the sets of interest leads to

$$\min \text{ diff}\left(\mathbb{Y}_1^{(2)}, \mathbb{X}_1^{(2)}\right) = (N_1+1)-(1+2B_1)-(1+2A_1)$$

$$= \begin{cases} 4r-1-2(r-1+r), & \text{if } N_1 = 4r, \\ 4r+1-1-2(r-1+r), & \text{if } N_1 = 4r+1, \\ 4r+2-1-2(r-1+r+1), & \text{if } N_1 = 4r+2, \\ 4r+3-1-2(r+r), & \text{if } N_1 = 4r+3. \end{cases}$$

$$= \begin{cases} 1, & \text{if } N_1 \text{ is even,} \\ 2, & \text{if } N_1 \text{ is odd,} \end{cases} \tag{16}$$

$$\min \text{ diff}\left(\mathbb{X}_2^{(2)}, \mathbb{Y}_1^{(2)}\right) = (N_1+3)-(N_1) = 3, \tag{17}$$

$$\min \text{ diff}\left(\mathbb{Y}_2^{(2)}, \mathbb{X}_2^{(2)}\right)$$

$$= (2(N_1+1)-(2+2B_2))-((N_1+1)+(2+2A_2))$$

$$= \begin{cases} 3, & \text{if } N_1 \text{ is even,} \\ 2, & \text{if } N_1 \text{ is odd,} \end{cases} \tag{18}$$

$$\min \text{ diff}\left(\{2(N_1+1)\}, \mathbb{Y}_2^{(2)}\right)$$

$$= 2(N_1+1)-(2(N_1+1)-2) = 2, \tag{19}$$

$$\text{diff}\left(\{N_2(N_1+1)\}, \mathbb{Z}_2^{(2)}\right) = 1. \tag{20}$$

Furthermore, since the sets $\mathbb{X}_1^{(2)}, \mathbb{Y}_1^{(2)}, \mathbb{X}_2^{(2)}$, and $\mathbb{Y}_2^{(2)}$ are ULAs with sensor separation 2, their cross differences are also ULAs

with separation 2. Applying this property to (16) gives

$$\text{The second smallest element of diff}\left(\mathbb{Y}_1^{(2)}, \mathbb{X}_1^{(2)}\right), \text{ if exists,}$$
$$= \begin{cases} 3, & \text{if } N_1 \text{ is even,} \\ 4, & \text{if } N_1 \text{ is odd.} \end{cases} \tag{21}$$

Now it is clear to determine the weight functions $w(m)$ for $m = 1, 2, 3$, based on (15) to (21). For $m = 1$, the sensor pairs of separation 1 only occur at (16) and (20), while (15), (17), (18), (19), and (21) do not contribute to $w(1)$. This argument proves the $w(1)$ part. When $m = 2$, the associated sensor pairs can be found in (15), (16), (18), and (19). Therefore, $w(2)$ can be expressed as

$$w(2) = \begin{cases} 1 + \sum_{q=1}^{2} (A_q)_+ + (B_q)_+ & \text{if } N_1 \text{ is even,} \\ 3 + \sum_{q=1}^{2} (A_q)_+ + (B_q)_+ & \text{if } N_1 \text{ is odd.} \end{cases}$$
$$= \begin{cases} N_1 - 3, & \text{if } N_1 \text{ is even,} \\ N_1 - 1, & \text{if } N_1 \text{ is odd.} \end{cases}$$

If $m = 3$, we first consider the case when N_1 is even. When $N_1 = 4$, we obtain the following sets

$$\mathbb{X}_1^{(2)} = \{1, 3\}, \mathbb{Y}_1^{(2)} = \{4\}, \mathbb{X}_2^{(2)} = \{7\}, \mathbb{Y}_2^{(2)} = \emptyset,$$

where $\emptyset$ denotes the empty set. Besides, the minimum element in $\mathbb{Z}_1^{(2)}$ is $2(N_1 + 1) = 10$. Counting these differences directly gives $w(3) = 3$. When $N_1 = 6$, these sets become

$$\mathbb{X}_1^{(2)} = \{1, 3, 5\}, \mathbb{Y}_1^{(2)} = \{6\}, \mathbb{X}_2^{(2)} = \{9, 11\}, \mathbb{Y}_2^{(2)} = \emptyset,$$

and $2(N_1 + 1) = 14$ so $w(3) = 3$.

If $N_1 \geq 8$ and N_1 is an even number, then $\mathbb{X}_1^{(2)}$ has at least three elements, $\mathbb{Y}_1^{(2)}$ has at least two elements, and $\mathbb{Y}_2^{(2)}$ is non-empty. In this case, the sensor pairs with separation 3 can be found in (17) and (18). Furthermore, the sensor pairs with separation 3 in (21) are

$$\text{Pair } \#1 : ((N_1 + 1) - (1 + 2B_1)) - (1 + 2(A_1 - 1)) = 3,$$

$$\text{Pair } \#2 : ((N_1 + 1) - (1 + 2(B_1 - 1))) - (1 + 2A_1) = 3.$$

Therefore $w(3) = 4$ if $N_1 \geq 8$ and N_1 is even.

When N_1 is odd, the only sensor pair leading to $w(3)$ is shown in (17), which completes the proof. ■

Summarizing this section, super nested arrays are generalizations of nested arrays. First of all, there is a simple closed-form expression for sensor locations, as in the case of nested and coprime arrays (and unlike MRAs). Second, for a fixed number of sensors, the physical aperture and the difference coarray are exactly identical to those of nested arrays, so that the DOF for DOA estimation remains unchanged. In particular, there are no holes in the coarray unlike coprime arrays. Finally, as in coprime arrays, the mutual coupling effects are much less severe than in nested arrays, because the sensors in the dense ULA part of the nested array have now been redistributed. In short, the super nested array combines the best features of nested and coprime arrays.

VI. Numerical Examples

In this section, we select six array configurations: ULA, MRA, nested arrays, coprime arrays, second-order super nested arrays, as well as third-order super nested arrays,[1] and then compare their performance in the presence of mutual coupling. The number of sensors is fixed to be 14. The sensor locations for MRA are given by [31][2]

$$\mathbb{S}_{\text{MRA}} = \{0, 1, 6, 14, 22, 30, 38, 46, 54, 56, 58, 61, 63, 65\}.$$

For nested arrays and super nested arrays, we set $N_1 = N_2 = 7$. For coprime arrays, we choose $M = 4$ and $N = 7$. The sensor locations are given by (6), (7) and Definition 7 so that there are $N_1 + N_2 = 14$ sensors for nested arrays as well as super nested arrays and $N + 2M - 1 = 14$ sensors for coprime arrays. If the central ULA part of the difference coarray of an array has $2P + 1$ elements, i.e., the uniform DOF is $2P + 1$, then P sources can be identified using the coarray MUSIC (SS-MUSIC) algorithm [16], [26]. In our case the nested and super nested arrays have a ULA for the coarray and the coprime array has a central ULA part and then some holes. It is readily verified that the number of identifiable sources in each case is as follows:

$$\text{ULA} : 13 \text{ sources.} \tag{22}$$

$$\text{MRA} : 65 \text{ sources.} \tag{23}$$

$$\text{Coprime array} : MN + M - 1 = 31 \text{ sources.} \tag{24}$$

$$\text{(Super) Nested array} : N_2(N_1 + 1) - 1 = 55 \text{ sources.} \tag{25}$$

It is well-known that the array aperture affects the estimation performance [38]–[40]. Larger array aperture tends to have finer spatial resolution and smaller estimation error. However, it suffices to consider the uniform DOF rather than the array aperture, since the uniform DOF is approximately twice the array aperture for restricted arrays. For instance, consider a physical array whose sensors are located at 0, 1, 4, 6, in units of $\lambda/2$. Then, the array aperture is 6 and the difference coarray $\mathbb{D} = \{-6, ..., 6\}$. The uniform DOF is $13 = 2 \times 6 + 1$, which is about twice the array aperture 6. Therefore, in what follows, we focus on the uniform DOF, rather than the array aperture, to explain the overall estimation performance.

A. Weight Functions and Mutual Coupling Matrices

The first example compares weight functions and the associated mutual coupling matrix (10). We choose $c_1 = 0.3e^{j\pi/3}$ and $B = 100$. The remaining coupling coefficients are given by $c_\ell = c_1 e^{-j(\ell-1)\pi/8}/\ell$ for $2 \leq \ell \leq B$. The first row of Fig. 7 shows the weight functions $w(m)$. In nested arrays, the associated weight function possesses a triangular region in the center, due to the dense ULA part. This triangular region breaks into smaller ones in the second-order super nested array $(w(1) = 1, w(2) = 6, w(3) = 1$, as in Theorem 2) and the third-order super nested array $(w(1) = 1, w(2) = 3, w(3) = 2)$. Coprime arrays exhibit

[1] Higher order super nested arrays will be introduced in the companion paper [37], and have even better performance. Here we include an example just for completeness of comparison.

[2] Strictly speaking, this array only gets close to the minimum redundancy (or equivalently maximum uniform DOF), rather than achieving the optimal one. However, it is still called MRA in [31].

smaller weight functions ($w(1) = w(2) = w(3) = 2$, as in (14)) than those of nested arrays ($w(1) = 7, w(2) = 6, w(3) = 5$, as in (13)).

The quantity $|[\mathbf{C}]_{i,j}|^2$, where $\mathbf{C}$ is the mutual coupling matrix, is shown in log-scale on the second row of Fig. 7. The darker region indicates less energy in the corresponding entry. It can be seen that all these $\mathbf{C}$ matrices are nearly-diagonal. In particular, $\mathbf{C}$ is a symmetric Toeplitz matrix for ULA. Note that if $\mathbf{C}$ is a diagonal matrix, sensor responses do not interfere with each other so it is free from mutual coupling. Hence, the energy of the off-diagonal components characterizes the amount of mutual coupling. We define the *coupling leakage* L as

$$L = \frac{\| \mathbf{C} - \text{diag}(\mathbf{C}) \|_F}{\| \mathbf{C} \|_F},$$

where $[\text{diag}(\mathbf{C})]_{i,j} = [\mathbf{C}]_{i,j}\delta_{i,j}$ and $\| \cdot \|_F$ denotes the Frobenius norm of a matrix. It is clear that $0 \leq L \leq 1$. Conceptually speaking, the smaller L is, the less the mutual coupling is. According to the third row of Fig. 7, the ULA suffers from the most severe mutual coupling effect. The third-order super nested array possesses the least L, suggesting it might have the least mutual coupling effect. In addition, high-order super nested arrays reduce the mutual coupling effect of their parent nested arrays, which can be inferred from the coupling leakage L among the nested array, the second-order super nested array, and the third-order one.

B. MUSIC Spectra in the Presence of Mutual Coupling

The second part of the simulation investigates the associated MUSIC spectra under various array configurations. The number of snapshots is 500 while the SNR is 0 dB. The measurement vector $\mathbf{x}_{\mathbb{S}}$ is contaminated by the mutual coupling matrix $\mathbf{C}$ and the MUSIC spectrum $P(\bar{\theta})$ is evaluated directly from $\mathbf{x}_{\mathbb{S}}$ *without using any decoupling algorithms*. Note that these results can be further improved by a variety of decoupling algorithms [6], [11]–[13], [35]. Our setting provides a baseline performance for different arrays. We will show that, even without decoupling, super nested arrays are still able to perform DOA estimation within reasonable amount of error.

Fig. 8 shows the MUSIC spectra when $D = 10$ sources are located at $\bar{\theta}_i = -0.1 + 0.2(i-1)/9$ for $i = 1, 2, ..., 10$, as indicated by the ticks and the vertical lines. This example examines the performance when the number of sources ($D = 10$) is less than the number of sensors 14. It is deduced from Fig. 8 that the ULA and the coprime array have false peaks, the nested array displays 11 peaks, while the MRA and the super nested arrays can resolve 10 true peaks. In terms of the estimation error E defined in (11), the best performance is exhibited by the third-order super nested array ($E = 0.00023647$), followed by the second-order super nested array ($E = 0.00042112$), then the MRA ($E = 0.00060242$), then the nested array ($E = 0.01216$), then the coprime array ($E = 0.12509$), and finally the ULA ($E = 0.17445$). It is noteworthy that the estimation error for the second-order super nested array is approximately 70% of that for the MRA, 3.5% of that for the nested array, and 0.3% of that for the coprime array. On the other hand, the RMSE for the third-order super nested array is roughly 40% of that for the MRA, only 2% of that for the nested array, and only 0.2% of that for the coprime array. To evaluate the RMSE, we use the root MUSIC algorithm [4] on the noise subspace to estimate DOAs. In the root MUSIC algorithm, suppose the roots on or inside the unit circle are denoted by $r_1, r_2, ..., r_D, r_{D+1}, ..., r_P$ such that $1 \geq |r_1| \geq |r_2| \geq \cdots \geq |r_D| \geq |r_{D+1}| \geq \cdots \geq |r_P|$. These DOAs are obtained from the phases of $r_1, r_2, ..., r_D$, which lead to D DOAs.

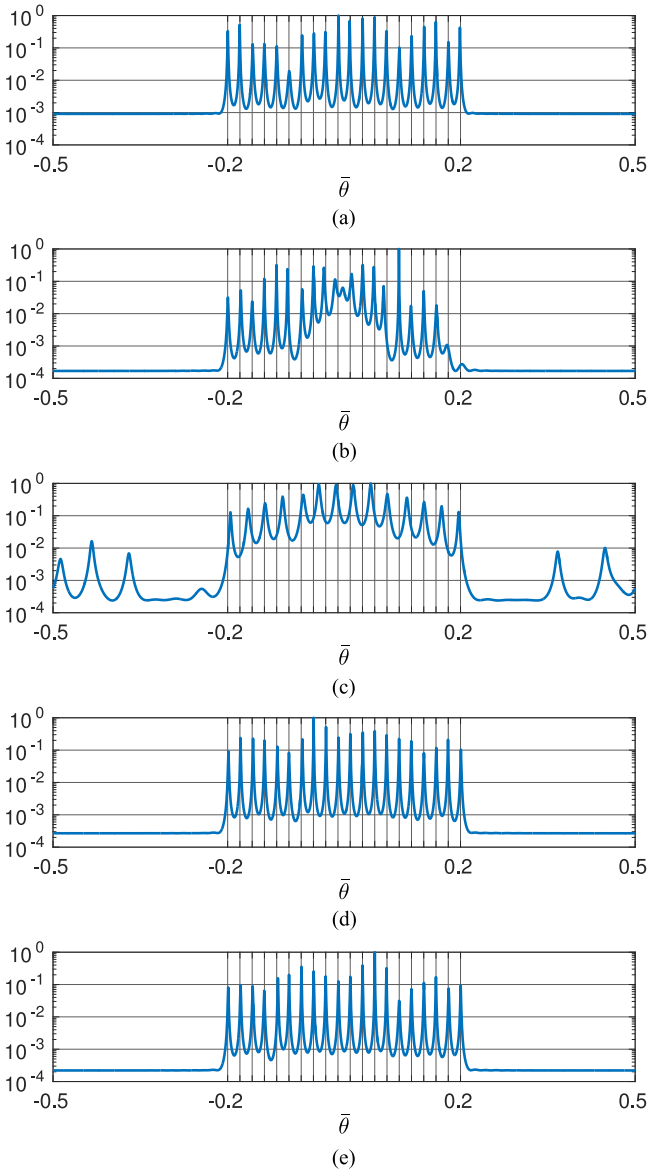

Fig. 9. The MUSIC spectra $P(\bar{\theta})$ for MRA, nested arrays, coprime arrays, second-order super nested arrays, and third-order super nested arrays when $D = 20$ sources are located at $\bar{\theta}_i = -0.2 + 0.4(i-1)/19, i = 1, 2, ..., 20$, as depicted by ticks and vertical lines. The SNR is 0 dB while the number of snapshots is $K = 500$. Note that the number of sources 20 is greater than the number of sensors 14. The mutual coupling is based on (10) with $c_1 = 0.3e^{j\pi/3}, B = 100$, and $c_\ell = c_1 e^{-j(\ell-1)\pi/8}/\ell$ for $2 \leq \ell \leq B$. (a) MRA, $D = 20, E = 0.00070437$. (b) Nested array, $D = 20, E = 0.015037$. (c) Coprime array, $D = 20, E = 0.12749$. (d) Second-order super nested, $D = 20, E = 0.00082022$. (e) Third-order super nested, $D = 20, E = 0.00071101$.

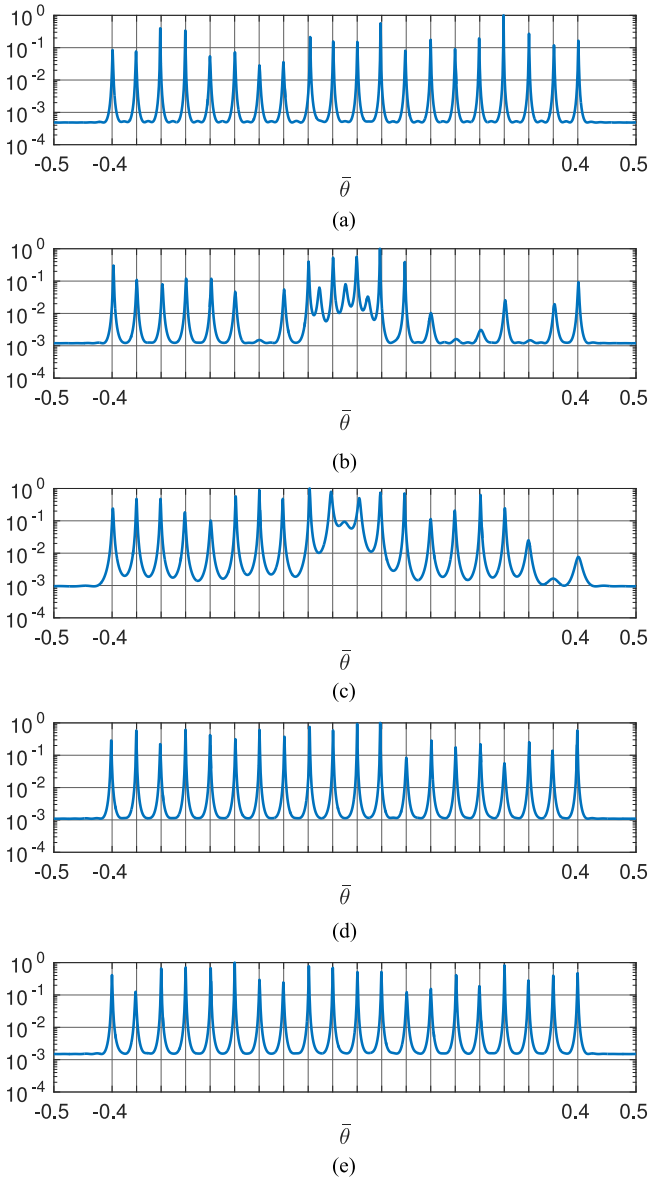

Fig. 10. The MUSIC spectra $P(\overline{\theta})$ for MRA, nested arrays, coprime arrays, second-order super nested arrays, and third-order super nested arrays when $D = 20$ sources are located at $\overline{\theta}_i = -0.4 + 0.8(i-1)/19, i = 1, 2, ..., 20$, as depicted by ticks and vertical lines. The SNR is 0 dB while the number of snapshots is $K = 500$. The mutual coupling is based on (10) with $c_1 = 0.3e^{j\pi/3}, B = 100$, and $c_\ell = c_1 e^{-j(\ell-1)\pi/8}/\ell$ for $2 \le \ell \le B$. (a) MRA, $D = 20, E = 0.0012123$. (b) Nested array, $D = 20, E = 0.04245$. (c) Coprime array, $D = 20, E = 0.027151$. (d) Second-order super nested, $D = 20, E = 0.0011955$. (e) Third-order super nested, $D = 20, E = 0.00073657$.

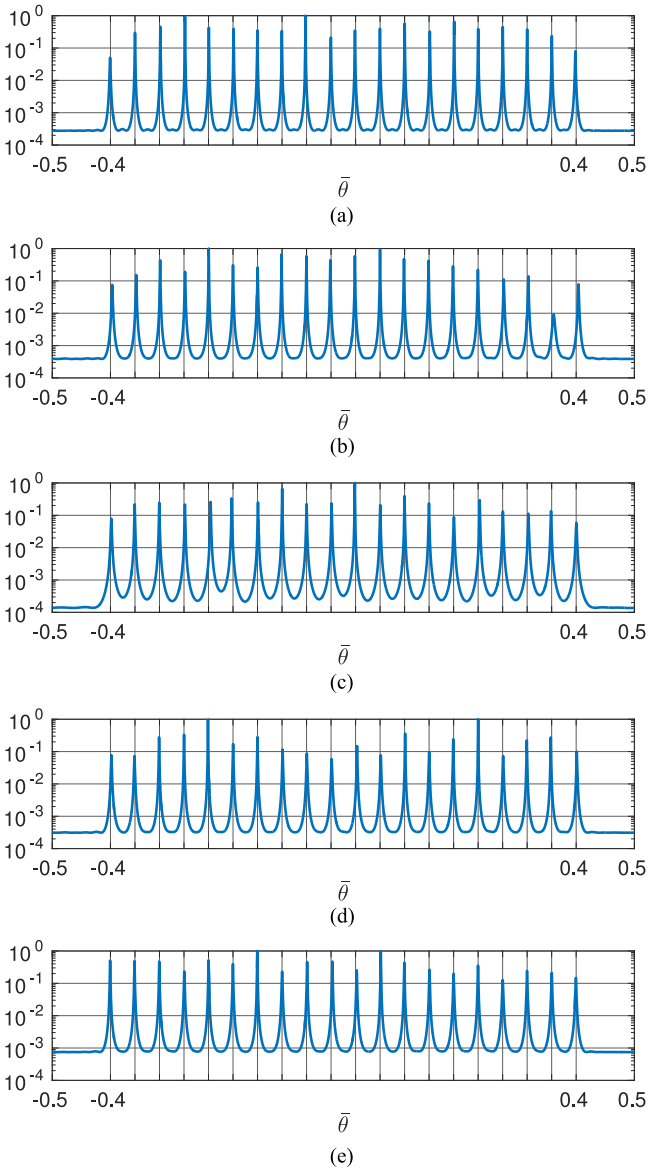

Fig. 11. Based on the practical mutual coupling model (9), the MUSIC spectra $P(\overline{\theta})$ are listed for MRA, nested arrays, coprime arrays, second-order super nested arrays, and third-order super nested arrays, where $D = 20$ sources are located at $\overline{\theta}_i = -0.4 + 0.8(i-1)/19, i = 1, 2, ..., 20$. The SNR is 0 dB while the number of snapshots is $K = 500$. The parameters in (9) are given by $Z_A = Z_L = 50$ and $l = \lambda/2$. (a) MRA, $D = 20, E = 0.00091204$. (b) Nested array, $D = 20, E = 0.0017399$. (c) Coprime array, $D = 20, E = 0.0014204$. (d) Second-order super nested, $D = 20, E = 0.0010173$. (e) Third-order super nested, $D = 20, E = 0.00083662$.

Fig. 9 lists another experiment with $D = 20$ sources, where D exceeds the number of sensors 14. These sources are located at $\overline{\theta}_i = -0.2 + 0.4(i-1)/19$, where $i = 1, 2, ..., 20$. The ULA fails to distinguish 20 sources due to (22). The MRA and the super nested arrays are capable of distinguishing 20 sources while the nested array (21 peaks) and the coprime array (with false peaks) are not. Among those resolving true DOAs, the best performance is exhibited by MRA $(E = 0.00070437)$, followed by the third-order super nested array $(E = 0.00071101)$, and then the second-order super nested array $(E = 0.00082022)$.

The reason why the ranking is different for large D is this: when D is small, the performance depends mostly on the mutual coupling, so the super nested arrays perform better than MRA. But as D gradually increases and gets closer to the upper limit of super nested arrays (55, as in (25)), which is smaller than the upper limit for MRA (65, as in (23)), this degrades the performance of super nested arrays before it begins to affect MRA.

Fig. 10 plots the MUSIC spectra for $D = 20$ equal-power, uncorrelated sources. These sources are more widely

separated, compared to those in Fig. 9. The true normalized DOAs are $\overline{\theta}_i = -0.4 + 0.8(i-1)/19, i = 1, 2, ..., 20$. Hence, based on Section III, the mutual coupling (or the weight functions) becomes more significant than the uniform DOF (or the spatial resolution). The least RMSE is now enjoyed by the third-order super nested array $(E = 0.00073657)$, followed by the second-order super nested array $(E = 0.0011955)$, then the MRA $(E = 0.0012123)$, then the coprime array $(E = 0.027151)$, and finally the nested array $(E = 0.04245)$. It can be observed that the coprime array, in this example, is more satisfactory than the nested array. There is only one spurious peak in the coprime array, as in Fig. 10(c), while many spurious peaks and missing targets exist in the nested array, as shown in Fig. 10(b). It is because the coprime array has reduced mutual coupling $(w(1) = w(2) = w(3) = 2$, as in (14)), in comparison of the nested array $(w(1) = 7, w(2) = 6, w(3) = 5$, as in (13)), even though the uniform DOF of the coprime array is smaller than that of the nested array.

Fig. 11 considers the MUSIC spectra under the linear dipole model for mutual coupling, (9), which is more practical than (10). For the mutual coupling model (9), the parameters Z_A and Z_L are 50 ohms while the dipole length $l = \lambda/2$. The source locations are identical to those in Fig. 10. In this scenario, the best estimation performance is exhibited by the third-order super nested array $(E = 0.00083662)$, followed by the MRA $(E = 0.00091204)$, then the second-order super nested array $(E = 0.0010173)$, then the coprime array $(E = 0.0014204)$, and finally the nested array $(E = 0.0017399)$. It can be observed that all these sparse arrays are capable of identifying 20 sources. This phenomenon is due to the following: First, the sources are widely separated and $D = 20$ is less than the maximum number of identifiable sources, as shown in (23) to (25). Second, the estimation performance depends on the mutual coupling model and the choice of parameters. In this specific example, the mutual coupling effect in Fig. 11 is less severe than that in Fig. 10 so that all these sparse arrays are able to resolve the sources correctly.

VII. Concluding Remarks

In this paper, we introduced super nested arrays. These share many of the good properties of nested arrays but at the same time, have reduced mutual coupling effects. For a fixed number of sensors, the super nested array has the same aperture and the same coarray as the parent nested array. Therefore, the DOF for DOA estimation is unchanged, while at the same time the effects of mutual coupling are reduced. One future direction for further improvement would be to use these arrays in conjunction with techniques which decouple or compensate the effect of mutual coupling such as the ones in [6], [8], [10]–[15], [35].

Notice from Theorem 2 that, while the weights $w(1)$ and $w(3)$ are significantly smaller than that of the parent nested array, the weight $w(2)$ is only slightly improved. How can we modify the array configuration further so that $w(2)$ is also decreased significantly without noticeably penalizing $w(1)$ and $w(2)$? The answer lies in the Qth-order super nested array which is introduced and studied in considerable detail in the companion paper [37].

Acknowledgment

P. P. Vaidyanathan wishes to thank Prof. Moeness Amin and his group at Villanova University for discussion on reduction of effects of mutual coupling, by using optimization methods in the estimation of $\mathbf{C}$ and the DOAs [35]. Although the work in [35] does not overlap with our work, [35] inspired us to develop arrays with smaller mutual coupling.

References

[1] M. I. Skolnik, *Introduction to Radar Systems*, 3rd ed. New York, NY, USA: McGraw Hill, 2001.
[2] S. Haykin, *Array Signal Processing*. Englewood Cliffs, NJ, USA: Prentice-Hall, 1984.
[3] L. Godara, "Application of antenna arrays to mobile communications, Part II: Beam-forming and direction-of-arrival considerations," *Proc. IEEE*, vol. 85, no. 8, pp. 1195–1245, Aug. 1997.
[4] H. L. Van Trees, *Optimum Array Processing: Part IV of Detection, Estimation, and Modulation Theory*. New York, NY, USA: Wiley-Interscience, 2002.
[5] C. A. Balanis, *Antenna Theory: Analysis and Design*, 4th ed. New York, NY, USA: Wiley, 2016.
[6] B. Friedlander and A. Weiss, "Direction finding in the presence of mutual coupling," *IEEE Trans. Antennas Propag.*, vol. 39, no. 3, pp. 273–284, Mar. 1991.
[7] H. T. Hui, "Decoupling methods for the mutual coupling effect in antenna arrays: A review," *Recent Patents Eng.*, vol. 1, pp. 187–193, 2007.
[8] K. Pasala, "Mutual coupling effects and their reduction in wideband direction of arrival estimation," *IEEE Trans. Aerosp. Electron. Syst.*, vol. 30, no. 4, pp. 1116–1122, Oct. 1994.
[9] H. Hui, "Improved compensation for the mutual coupling effect in a dipole array for direction finding," *IEEE Trans. Antennas Propag.*, vol. 51, no. 9, pp. 2498–2503, Sep. 2003.
[10] T. Svantesson, "Modeling and estimation of mutual coupling in a uniform linear array of dipoles," in *Proc. IEEE Int. Conf. Acoust. Speech Signal Process.*, 1999, vol. 5, pp. 2961–2964.
[11] T. Svantesson, "Mutual coupling compensation using subspace fitting," in *Proc. IEEE Sensor Array Multichannel Signal Process. Workshop*, 2000, pp. 494–498.
[12] M. Lin and L. Yang, "Blind calibration and DOA estimation with uniform circular arrays in the presence of mutual coupling," *IEEE Antennas Wireless Propag. Lett.*, vol. 5, no. 1, pp. 315–318, Dec. 2006.
[13] F. Sellone and A. Serra, "A novel online mutual coupling compensation algorithm for uniform and linear arrays," *IEEE Trans. Signal Process.*, vol. 55, no. 2, pp. 560–573, Feb. 2007.
[14] Z. Ye, J. Dai, X. Xu, and X. Wu, "DOA estimation for uniform linear array with mutual coupling," *IEEE Trans. Aerosp. Electron. Syst.*, vol. 45, no. 1, pp. 280–288, Jan. 2009.
[15] J. Dai, D. Zhao, and X. Ji, "A sparse representation method for DOA estimation with unknown mutual coupling," *IEEE Antennas Wireless Propag. Lett.*, vol. 11, pp. 1210–1213, 2012.
[16] P. Pal and P. P. Vaidyanathan, "Nested arrays: A novel approach to array processing with enhanced degrees of freedom," *IEEE Trans. Signal Process.*, vol. 58, no. 8, pp. 4167–4181, Aug. 2010.
[17] P. P. Vaidyanathan and P. Pal, "Sparse sensing with co-prime samplers and arrays," *IEEE Trans. Signal Process.*, vol. 59, no. 2, pp. 573–586, Feb. 2011.
[18] S. Qin, Y. Zhang, and M. Amin, "Generalized coprime array configurations for direction-of-arrival estimation," *IEEE Trans. Signal Process.*, vol. 63, no. 6, pp. 1377–1390, Mar. 2015.
[19] Z. Tan, Y. Eldar, and A. Nehorai, "Direction of arrival estimation using co-prime arrays: A super resolution viewpoint," *IEEE Trans. Signal Process.*, vol. 62, no. 21, pp. 5565–5576, Nov. 2014.
[20] K. Adhikari, J. R. Buck, and K. E. Wage, "Extending coprime sensor arrays to achieve the peak side lobe height of a full uniform linear array," *EURASIP J. Adv. Signal Process.*, vol. 2014, no. 1, 2014.
[21] A. T. Moffet, "Minimum-redundancy linear arrays," *IEEE Trans. Antennas Propag.*, vol. 16, no. 2, pp. 172–175, 1968.
[22] H. Taylor and S. W. Golomb, "Rulers, Part I," Univ. Southern Calif., Los Angeles, CA, USA, Tech. Rep. 85-05-01, 1985.
[23] E. Vertatschitsch and S. Haykin, "Nonredundant arrays," *Proc. IEEE*, vol. 74, no. 1, pp. 217–217, Jan. 1986.

[24] J. Leech, "On the representation of $1, 2, \ldots, n$ by differences," *J. London Math. Soc.*, vol. 1, no. 2, pp. 160–169, 1956.
[25] [Online]. Available: http://systems.caltech.edu/dsp/students/clliu/SuperNested/SN.zip
[26] P. Pal and P. P. Vaidyanathan, "Coprime sampling and the MUSIC algorithm," in *Proc. IEEE Dig. Signal Process. Educ. Workshop*, Jan. 2011, pp. 289–294.
[27] C.-L. Liu and P. P. Vaidyanathan, "Remarks on the spatial smoothing step in coarray MUSIC," *IEEE Signal Process. Lett.*, vol. 22, no. 9, pp. 1438–1442, Sept. 2015.
[28] Y. Abramovich, D. Gray, A. Gorokhov, and N. Spencer, "Positive-definite Toeplitz completion in DOA estimation for nonuniform linear antenna arrays–Part I: Fully augmentable arrays," *IEEE Trans. Signal Process.*, vol. 46, no. 9, pp. 2458–2471, Sept. 1998.
[29] Y. Abramovich, N. Spencer, and A. Gorokhov, "Positive-definite Toeplitz completion in DOA estimation for nonuniform linear antenna arrays–Part II: Partially augmentable arrays," *IEEE Trans. Signal Process.*, vol. 47, no. 6, pp. 1502–1521, Jun. 1999.
[30] P. Pal and P. P. Vaidyanathan, "Correlation-aware techniques for sparse support recovery," in *Proc. IEEE Stat. Signal Process. Workshop*, Aug. 2012, pp. 53–56.
[31] M. Ishiguro, "Minimum redundancy linear arrays for a large number of antennas," *Radio Sci.*, vol. 15, no. 6, pp. 1163–1170, 1980.
[32] H. King, "Mutual impedance of unequal length antennas in echelon," *IRE Trans. Antennas Propag.*, vol. 5, no. 3, pp. 306–313, Jul. 1957.
[33] T. Svantesson, "Direction finding in the presence of mutual coupling," M.S. thesis, Chalmers Univ. Technol., Chalmers, Sweden, 1999.
[34] H. S. Lui and H. T. Hui, "Mutual coupling compensation for direction-of-arrival estimations using the receiving-mutual-impedance method," *Int. J. Antennas Propag.*, vol. 2010, 2010, article ID. 373061.
[35] E. BouDaher, F. Ahmad, M. G. Amin, and A. Hoorfar, "DOA estimation with co-prime arrays in the presence of mutual coupling," in *Proc. Eur. Signal Process. Conf.*, Nice, France, 2015, pp. 2830–2834.
[36] B. Friedlander, "A sensitivity analysis of the MUSIC algorithm," *IEEE Trans. Acoust. Speech Signal Process.*, vol. 38, no. 10, pp. 1740–1751, Oct. 1990.
[37] C.-L. Liu and P. P. Vaidyanathan, "Super nested arrays: Linear sparse arrays with reduced mutual coupling–Part II: High-order extensions," *IEEE Trans. Signal Process.*, 2016, DOI: 10.1109/TSP.2016.2558167.
[38] P. Stoica and A. Nehorai, "MUSIC, maximum likelihood, and Cramer-Rao bound," *IEEE Trans. Acoust. Speech Signal Process.*, vol. 37, no. 5, pp. 720–741, May 1989.
[39] C. Chambers, T. Tozer, K. Sharman, and T. Durrani, "Temporal and spatial sampling influence on the estimates of superimposed narrowband signals: When less can mean more," *IEEE Trans. Signal Process.*, vol. 44, no. 12, pp. 3085–3098, Dec. 1996.
[40] P. P. Vaidyanathan and P. Pal, "Direct-MUSIC on sparse arrays," in *Proc. Int. Conf. Signal Process. Commun.*, Jul. 2012.

Chun-Lin Liu (S'12) was born in Yunlin, Taiwan, on April 28, 1988. He received the B.S. and M.S. degrees in electrical engineering and communication engineering from the National Taiwan University (NTU), Taipei, Taiwan, in 2010 and 2012, respectively. He is currently pursuing the Ph.D. degree in electrical engineering at the California Institute of Technology (Caltech), Pasadena, CA, USA.

His research interests are in sparse array processing, sparse array design, tensor signal processing, and filter bank design.

Mr. Liu was a recipient of the Best Student Paper Award at the 41st IEEE International Conference on Acoustics, Speech and Signal Processing, 2016, in Shanghai, China.

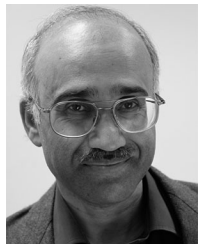

P. P. Vaidyanathan (S'80–M'83–SM'88–F'91) was born in Calcutta, India, on October 16, 1954. He received the B. Sc. (honors) degree in physics and the B. Tech. and M. Tech. degrees in radiophysics and electronics all from the University of Calcutta, India, in 1974, 1977 and 1979, respectively, and the Ph.D. degree in electrical and computer engineering from the University of California at Santa Barbara, Santa Barbara, CA, USA, in 1982.

He was a Postdoctoral Fellow at the University of California Santa Barbara from September 1982 to March 1983. In March 1983, he joined the Electrical Engineering Department, California Institute of Technology, Pasadena, CA, USA, as an Assistant Professor, and since 1993, he has been Professor of Electrical Engineering there. He has authored nearly 500 papers in journals and conferences, and is the author/coauthor of four books: *Multirate Systems and Filter Banks* (Englewood Cliffs, NJ, USA: Prentice-Hall, 1993), *Linear Prediction Theory* (London, U.K.: Morgan and Claypool, 2008), *Signal Processing and Optimization for Transceiver Systems* (Cambridge, U.K.: Cambridge Univ. Press, 2010, with Phoong and Lin), and *Filter Bank Transceivers for OFDM and DMT Systems* (Cambridge, U.K.: Cambridge Univ. Press, 2010). He has written several chapters for various signal processing handbooks. His main research interests are in digital signal processing, multirate systems, wavelet transforms, signal processing for digital communications, genomic signal processing, radar signal processing, and sparse array signal processing.

Dr. Vaidyanathan served as Vice-Chairman of the Technical Program Committee for the 1983 IEEE International Symposium on Circuits and Systems, and as the Technical Program Chairman for the 1992 IEEE International Symposium on Circuits and Systems. He was an Associate Editor for the IEEE TRANSACTIONS ON CIRCUITS AND SYSTEMS in 1985–1987, and is currently an Associate Editor for IEEE SIGNAL PROCESSING LETTERS, and a consulting editor for *Applied and Computational Harmonic Analysis*. In 1998, he was a guest editor of special issues on topics of filter banks, wavelets, and subband coders in the IEEE TRANSACTIONS ON SIGNAL PROCESSING and the IEEE TRANSACTIONS ON CIRCUITS AND SYSTEMS II. He was a recipient of the Award for Excellence in Teaching at the California Institute of Technology for 1983–1984, 1992–1993 and 1993–1994. He also received the NSF's Presidential Young Investigator Award in 1986. In 1989, he received the IEEE ASSP Senior Award for his paper on multirate perfect-reconstruction filter banks. In 1990, he was a recipient of the S. K. Mitra Memorial Award from the Institute of Electronics and Telecommunications Engineers, India, for his joint paper in the *IETE Journal*. In 2009, he was chosen to receive the IETE students– journal award for his tutorial paper in the *IETE Journal of Education*. He was also the coauthor of a paper on linear-phase perfect reconstruction filter banks in the IEEE TRANSACTIONS ON SIGNAL PROCESSING, for which the first author (T. Nguyen) received the Young outstanding author award in 1993. He received the 1995 F. E. Terman Award of the American Society for Engineering Education, sponsored by Hewlett Packard Co., for his contributions to engineering education. He has given several plenary talks on signal processing including at the IEEE ISCAS–04, Sampta–01, Eusipco–98, SPCOM–95, and Asilomar–88 conferences. He has been chosen a Distinguished Lecturer for the IEEE Signal Processing Society for 1996–1997. In 1999, he was chosen to receive the IEEE CAS Society's Golden Jubilee Medal. He is a recipient of the IEEE Signal Processing Society's Technical Achievement Award for 2002, and the IEEE Signal Processing Society's Education Award for 2012. He is a recipient of the IEEE Gustav Kirchhoff Award (an IEEE Technical Field Award) in 2016, for "fundamental contributions to digital signal processing ". He also received the Northrup Grumman Excellence in Teaching Award for 2016.